Studies on Caspase-dependent Signaling Mechanism

Kouhei Shimizu

2013

Contents

PREFACE

Caspases (Cysteine-ASPartic-acid-proteASE) are a family of cysteine proteases with unique specificity, which play a critical role in apoptosis. The caspase gene family consists of 14 mammalian members that are grouped into two major sub-families: apoptotic and inflammatory caspases. The apoptotic caspases are further subdivided into two sub-groups, initiator caspases (e.g., caspase-2, -8, -9, -10) and effector caspases (caspase-3, -6, -7). The caspases are originally present as poorly active (initiator caspases) or inactive (effector caspases) precursor forms that can be proteolytically cleaved in order to be activated depending on the cellular context. Initiator caspases have a long N-terminal prodomain, which mediates the formation of protein complexes that provide the molecular platform for self-activation. Activation of initiator caspases predominantly occurs through death receptors as extrinsic signaling pathways or mitochondria and ER as intrinsic signaling pathways. Activated initiator caspases cleave specific substrates, including effector caspase zymogens. This process leads to activation of the effector caspases, which in turn cleave their substrates to execute apoptotic cell death. Thus, apoptosis orchestrated by caspases requires the action of many substrates that participate in apoptotic signaling.

Apoptosis, a form of programmed cell death, is indispensable for multicellular organisms, because the fundamental cellular response of apoptosis plays a crucial role in morphogenesis during development and in regulating tissue homeostasis by eliminating unwanted cells. Therefore, defects in the apoptotic program are implicated in a variety of diseases such as maldevelopment, tumorigenesis, neurodegeneration disease and autoimmune disease, indicating that components of caspase-dependent signaling pathway could be expected as potential therapeutic targets.

The caspase-dependent apoptotic signaling is finely tuned by multiple events such as direct phosphorylation of caspases, whereas protein kinases are often substrates of active caspases, especially caspase-3. In healthy cells, caspases are turned off by phosphorylation-mediated suppression in addition to other mechanisms. However, caspases are turned on to cleave protein kinases whenever cells receive a substantial stimulus that overcomes inhibitory mechanisms.

The caspase-mediated cleavage of protein kinases can terminate prosurvival signaling (e.g., loss of Akt kinase activity) or generate proapoptotic protein (e.g., cleaved ROCK1 and cleaved MST1). In this way, it seems that cross-regulation of caspases and protein kinases allows for fine-tuning of the apoptotic threshold. Thus, illustrating the relationships between caspases and their substrate protein kinases would help clarify the signal transduction events that occur during apoptosis, and understanding how the balance between cell survival and cell death can be regulated through the crosstalk would be of great biological and medical importance.

Although comprehensive identification of caspase substrates is absolutely essential to clarify the whole picture of caspase-dependent signaling, in complex biological samples, it could be limited by conventional proteomic approaches such as mass spectrometry owing to its property. For example, cellular protein expression levels may give bias to data accuracy. There is the possibility that the amount of many bona fide intracellular substrates is so small as to be undetectable. Furthermore, it is difficult to identify specific pairs of proteases and substrates because numerous cleavage events occur simultaneously in cells. Thus, an *in vitro* approach that could complement cell-based approaches is required. Prior to this doctoral thesis, we have developed a powerful screening method for identification of protease substrates using protein array produced by a wheat germ cell-free protein synthesis system and luminescence-based high-throughput detection technology for inter/intra molecular interactions. This method allowed us to identify 30 protein kinases as novel substrates for caspase-3 out of 304 kinases (Tadokoro et al: *Cell Death and Disease*, 2010).

It recently started to be recognized that caspase-dependent cleavage of selected substrates, especially protein kinases, contributes to not only apoptosis but also the regulation of cell differentiation. Hence, in this thesis, in an attempt to elucidate the regulatory mechanism of apoptosis and cell differentiation, among the above newly identified substrates, I investigated the role of TRB3 and Nek5 cleavages during the apoptotic and myogenic differentiation process, respectively.

CHAPTER I

Stress-inducible caspase substrate TRB3 promotes nuclear translocation of procaspase-3

SUMMARY

Pseudokinase TRB3 is a stress-inducible nuclear protein, which has recently been shown to be involved in ER stress-induced apoptosis. However, it remains unclear how TRB3 contributes to the process. We recently demonstrated that TRB3 was cleaved by caspase-3 (CASP3) *in vitro* and also in apoptosis-induced cells. Thus, I investigate the role of TRB3 cleavage in the apoptotic process to address the above question. Overexpression studies revealed that the cleavage of TRB3 promoted CASP3/7 activation and apoptosis. In contrast, the anti-apoptotic effects were found under TRB3 non-cleavable conditions, such as ER stress, and also when the CASP3/7 activation was enhanced by knockdown of endogenous TRB3 expression. Interestingly, nuclear translocation of procaspase-3 (proCASP3) was observed in cells either overexpressing TRB3 or under tunicamycin-induced ER stress. Although forced cytoplasmic expression of proCASP3 enhanced apoptosis significantly, its nuclear expression did not produce any pro-apoptotic effect, suggesting that nuclear distribution of proCASP3 is not critical for the execution of apoptosis. Thus, TRB3 might prevent cytoplasmic activation of CASP3 by promoting proCASP3 entry into the nucleus, and thereby inhibit apoptosis. Taken together, my results suggest that TRB3, through its own cleavage, functions as a molecular switch between the cell survival and apoptotic pathways under stressful conditions.

Abbreviations: CASP, caspase; CHX, cycloheximide; ER, endoplasmic reticulum; FRET, fluorescence resonance energy transfer; NLS, nuclear localization signal; Rb, retinoblastoma; TNFα, tumor necrosis factor-α; UPR, unfolded protein response; WT, wild type

1. INTRODUCTION

TRB3 (also known as TRIB3, NIPK, SINK, or SKIP), one of the mammalian orthologues of *Drosophila* Tribbles, was identified as a pseudokinase, because it contains a Ser/Thr protein kinase-like domain that lacked the ATP-binding domain and core catalytic residues, therefore, dose not have any kinase activity [1]. Despite a lack of characteristic functional domain, TRB3 has been shown to be involved in multiple cellular processes such as glucose and lipid metabolism, muscle and adipocyte differentiation, and stress response by interacting with various functional proteins (e.g. kinase: AKT, MAPK; transcription factor: ATF4, CHOP, PPARγ; E3 ubiquitin ligase: COP1) [2-9].

Endoplasmic reticulum (ER) stress has recently been recognized as another key pathway for triggering apoptosis [10,11]. The adaptive phase of ER stress promotes cell survival by reducing the accumulation of unfolded proteins through global transcriptional control, well known as the unfolded protein response (UPR) [12]. However, apoptosis is considered selected when the apoptotic pathway gains ascendancy over the adaptive pathway by overwhelming the ER stress. During ER stress, TRB3 is upregulated by an ER stress-inducible transcription factor, ATF4/CHOP [6]. Excess expression of TRB3 downregulates its own expression by negative feedback via the repression of ATF4/CHOP transcriptional activity [13]. Several studies suggest that CHOP and its transcriptional target, BH3-only proteins such as Bim and PUMA, promote ER stress-induced apoptosis [14,15]. TRB3 has been shown to be involved in ER stress-induced apoptosis via these regulatory processes [6,16]. TRB3 expression is also induced in a PI3K-dependent manner by nutrient deficiency, such as the lack of glucose or amino acids [17]. Results of a transient overexpression study suggest that TRB3 plays an apoptosis inhibitory role under glucose depletion condition. Thus, the expression of TRB3 could be both up- and down-regulated by various cellular stresses [18]. Taken together, these studies indicate that TRB3 functions as an important component of the stress response mechanism, namely, regulates stress-induced apoptosis. However, it remains to be elucidated how TRB3 contributes to the stress responses.

Caspase-3 (CASP3), one of the most downstream components of the caspase cascade, is

known to cleave many critical proteins such as lamin, PARP, ICAD/DFF45 and PAK2, and in turn induces irreversible apoptosis that involves substrate proteolysis and positive feedback of caspase cascade [19,20]. Recently, we have demonstrated that TRB3 is a substrate for CASP3 [21]. To investigate the role of TRB3 cleavage in the apoptotic process, I carried out cell-based analysis using the wild type and a non-cleavable mutant of TRB3. In this study, I have shown a TRB3 cleavage-dependent pro-apoptotic response, and have also presented evidence for a novel anti-apoptotic mechanism involving TRB3-mediated nuclear translocation of procaspase-3 (proCASP3). This dual function of TRB3 may serve as a key switch between the cell survival and apoptosis pathways depending on the cellular context.

2. MATERIALS AND METHODS

2.1. Plasmid constructions

Full-length human TRB3 cDNA and cDNA coding for amino acids 1-338 of human TRB3 (ΔC20-TRB3) were amplified by PCR. To construct the expression plasmids pcDNA3.1-V5-WT-TRB3 and pcDNA3.1-V5-ΔC20-TRB3, the above cDNAs were individually subcloned into the pcDNA3.1nV5-DEST vector (Invitrogen, Carlsbad, CA, USA) via the donor vector pDONR221 of the Gateway Cloning Technology kit (Invitrogen). An expression plasmid containing a cDNA of a caspase non-cleavable D338A mutant of TRB3 (pcDNA3.1-V5-D338A-TRB3) was generated from the pcDNA3.1-V5-WT-TRB3 plasmid by using the PrimeSTAR Mutagenesis Basal kit (TakaraBio, Otsu, Japan) and utilizing the mutagenic primers (5'-GTCCCTGCGGGACTGGGGCTGGACGAA-3' and 5'-CAGTCCCGCAGGGACCACCTGGGCAGC-3') as described in the manufacturer's instructions. In the same way, cDNAs of human caspase-3 and C163S mutant of caspase-3 (kindly provided by Dr. K. Sakamaki, Kyoto Univ.) were subcloned into the pcDNA6.2/C-EmGFP-DEST vector (Invitrogen) to construct the expression plasmids pcDNA6.2-proCASP3-EmGFP and pcDNA6.2-C163S-proCASP3-EmGFP, respectively. Three copies of the SV40 T-antigen nuclear localization signal (NLS) and HA tag sequences were fused by PCR to construct pcDNA6.2-proCASP3-NLS-EmGFP and pcDNA6.2-C163S-proCASP3-HA plasmids, respectively. The DsRed-NLS expression plasmid (pDsRed2-Nuc) was purchased from Clontech (Palo Alto, CA, USA).

2.2. In vitro cleavage assay

Construction of DNA templates and cell-free protein synthesis for N-terminal biotinylated-TRB3 were performed as described previously [21]. For the cleavage reaction, 3 μl of translation mixture was added to 7 μl of reaction mixture (20 mM HEPES, pH 7.8, 100 mM NaCl, 10 mM DTT, 1 mM EDTA, 10% sucrose), with 0.3 (CASP3, CASP7, CASP8), 10 (CASP9) or 20 (CASP2, CASP6, CASP10) units of each active caspase (1 unit is defined as the amount that will hydrolyze 1 nmole of the caspase substrate per minute or hour) (Sigma-Aldrich,

St. Louis, MO), and then the mixture was incubated for 2 hr at 30˚C. The assay using CASP9 was performed in the reaction mixture containing 10% PEG6000 because it is necessary for the CASP9 activity. Additionally, to remove PEG6000 from the reaction mixture after cleavage reaction, the biotinylated-TRB3 was recovered by streptavidin magnetic beads (Promega Corporation, Madison, WI, USA). These reaction mixture and recovered-TRB3 were boiled in SDS-PAGE sample buffer. The samples separated on SDS-PAGE were transferred to PVDF membrane (Millipore, Bedford, MA, USA). The membrane was probed with Alexa 488-conjugated streptavidin (Invitrogen), and then visualized using a Typhoon Imager (GE Healthcare, Piscataway, NJ).

2.3. Cell culture and transfection

HeLa and Jurkat cells were grown in Dulbecco's modified eagle medium (DMEM) and RPMI medium, respectively. Each medium was supplemented with 10% fetal bovine serum (FBS), 100 units/mL penicillin and 100 μg/mL streptomycin. Transient transfection of HeLa and Jurkat cells with plasmid was carried out using Lipofectamine 2000 (Invitrogen) and FuGENE6 (Roche, Indianapolis, IN, USA), respectively, and following the manufacturer's instructions. Empty vector pcDNA3.1 was used as a transfection control.

2.4. Apoptosis induction and assay

To induce apoptosis, cells were treated with TNFα/CHX [20 ng/mL TNFα (Calbiochem, La Jolla, CA), 100 μM CHX (Chemicon, Temecula, CA)], 125 ng/mL anti-Fas antibody (IgM, CH11) (Medical & Biological Laboratories Co., Ltd., Nagoya, Japan) or 5 μM tunicamycin (Sigma-Aldrich) for various times as indicated in the figure legends. For inhibition of apoptosis, the above reagents were supplemented with 100 μM z-VAD-FMK (Peptide Institute Inc., Osaka, Japan). DMSO was used as a treatment control. The treated cells were subjected to each assay or suspended in an equal volume of 0.5% trypan blue solution (Nacalai Tesque, Kyoto, Japan) for 1 min at room temperature, and then the stained cells were counted as dead cells.

2.5. Immunoblot analysis

After washing with PBS, cells were lysed in 2 × SDS-PAGE sample buffer (125 mM Tris-HC1, pH 6.8, 20% glycerol, 4% SDS, 10% 2-mercaptoethanol, 0.001% bromophenol blue) and the proteins in the cell lysates were heat denatured. Proteins in the cell lysates were separated by SDS-PAGE and then transferred to PVDF membrane (Millipore) by electroblotting. Membranes were subsequently used in immunoblot assay using one of the following primary antibodies: anti-V5 epitope (#R960-25, Invitrogen), anti-TRB3 (#2488-1, Epitomics, Burlingame, CA), and anti-α-tubulin (#T9026, Sigma-Aldrich). Chemiluminescent signals generated by Immobilon Western HRP substrate Luminol Reagent (Millipore) or ImmunoStar (Wako, Osaka, Japan), were detected using an LAS-4000 mini biomolecular imager (GE Healthcare).

2.6. Densitometric image analysis

To measure the relative expression level of proteins in cells, acquired images were densitometrically analyzed by using the ImageJ software (NIH, Bethesda, MD, USA).

2.7. Luminometric CASP3/7 activity assay

CASP3/7 activity was measured by using the luminometric Caspase-Glo® 3/7 Assay kit (Promega) and a GloMax™ 96 Microplate Luminometer (Promega) according to the manufacturer's instructions. CASP3/7 activity shown was relative to the untreated control value.

2.8. Knockdown of endogenous TRB3 by small interfering RNA and microRNA

Negative control siRNA (5'-AATTCTCCGAACGTGTCACGT-3') and siRNA oligonucleotide targeting 3'UTR of human TRB3 (5'-ATGAGGCTAGTTCTTGTCTAA-3') were purchased from QIAGEN (Valencia, CA, USA). Transfection of cells with siRNA was performed according to the manufacturer's instructions using TransIT-siQUEST transfection reagent (Mirus Bio Corporation, Madison, WI). For knockdown of human TRB3 using a miRNA interference, DNA duplexes targeting the TRB3 coding sequence (CDS)

(5'-TTGGAGTTGGATGACAACTTA-3') and 3'UTR (5'-CAGTTCCTGCTTGGGTGCTTA-3') were designed by using Invitrogen BLOCK-iT RNAi Designer (at www.invitrogen.com/rnaidesigner) and cloned into pcDNA6.2-GW/EmGFP-miR expression vector (Invitrogen) that enable identify artificial miRNA expressing cells by cocistronic expression of EmGFP. Negative control miRNA expression vector was purchased from Invitrogen.

2.9. Immunofluorescence analysis

HeLa cells grown on coverslips were washed with cold PBS, and then fixed with 2% paraformaldehyde in PBS for 10 min. After washing with PBS, the fixed cells were permeabilized with 0.5% Triton X-100 (Nacalai Tesque) in PBS for 5 min. After washing with PBS, the cells were incubated in a blocking buffer [TBS containing 5% calf serum (Invitrogen)] for 1 hr. The cells were then incubated with one of the primary antibodies (listed below) in TBST containing 0.05% BSA for 1 hr at 37˚C, washed three times with TBST (5 min each), and incubated with the Alexa Fluor 488/555-conjugated secondary antibody (Invitrogen) plus DAPI (Invitrogen) for 1 hr. After washing three times with TBST (5 min each), the stained cells were mounted on glass slides and visualized using a Carl Zeiss LSM710 confocal laser scanning microscope (Carl Zeiss, Jena, Germany). Primary antibodies: anti-V5 epitope (#R960-25, Invitrogen), anti-HA epitope (#11867423001, Roche), anti-Active-CASP3 (#9661, Cell Signaling Technology, Beverly, MA), and anti-TRB3 (#2488-1, Epitomics, Burlingame, CA).

2.10. Quantification of C163S-proCASP3-EmGFP and C163S-proCASP3-HA localization

Preferential localization of C163S-proCASP3-EmGFP in the fixed cells was assessed as either mainly cytoplasmic (C) or mainly nuclear (N) based on their observed relative fluorescence intensity using a Carl Zeiss LSM710 confocal laser scanning microscope. In a similar way, the localization of C163S-proCASP3-HA was also assessed in artificial miRNA expressing cells that could be assumed by cocistronic expression of EmGFP. To rule out the contribution of the active CASP3 to the quantification of proCASP3 localization, I examined

only morphologically normal cells (98.7% of tunicamycin-treated morphologically normal cells were active CASP3 negative; see text and Figure S5).

2.11. Live imaging analysis

Transfected HeLa cells grown on a glass bottom dish were set in the culture environment (37˚C, 5% CO_2) of microscope after treatment with a given agent. Images of EmGFP-fusion protein positive and DsRed positive cells, respectively, were acquired using the Carl Zeiss LSM710 confocal laser scanning microscope equipped with LSM 7 live module. Time-lapse images were taken with a 63 × plan apochromatic objective with a numerical aperture of 1.4. Each frame of time-lapse images was acquired every 5 minutes (Movie S1) or 10 minutes (Figure 4C) for the indicated times. Movie S1 was shown at 10 frames/sec.

2.12. Statistics

Data shown are mean ± S.D. Student's t test was used to determine the significance of differences. *P* values <0.05 were considered to be statistically significant.

3. RESULTS

3.1. TRB3 is cleaved by caspases in vitro and in the apoptotic process

We previously reported that TRB3 is cleaved by CASP3 at Asp338 [21]. To analyze the biological consequence of TRB3 cleavage by caspase, I constructed three recombinant plasmids for expressing the wild type (WT), CASP3 cleavage-site mutant (D338A) and CASP3-cleaved form (ΔC20) of TRB3, respectively, cartoon diagrams of which are shown in Figure 1A. As was shown in our previous report [21], the WT-TRB3 was cleaved by CASP3 *in vitro* (Figure 1B). In contrast, the D338A-TRB3 and ΔC20-TRB3 were not cleaved by CASP3. This result suggests that TRB3 was cleaved at a single site by CASP3. I also tested CASP2, CASP6, CASP7, CASP8, CASP9 and CASP10 for their ability to cleave TRB3 in this *in vitro* assay (Figure 1C). Surprisingly, all caspases used in this assay cleaved the WT-TRB3, and all of them, except for CASP2, were unable to cleave the D338A mutant. As judged from the mobility of the cleaved fragment on the SDS/PAGE (Figure 1C), the CASP2 cleavage site must be more close to the C-terminal end of TRB3 than the Asp338 residue, and I predicted that this site could be either at Asp343 and/or at Asp351. These results suggest that TRB3 is cleaved by multiple caspases, and the primary cleavage site is located at Asp338. Sequence alignment analysis of the TRB3 caspase-cleavage sites from multiple species raised a possibility that TRB3 is cleaved in various species and the cleavage has biological significance (see Figure S1 for details).

To examine whether TRB3 is cleaved in apoptosis-induced cells, I transfected HeLa and Jurkat cells separately with the recombinant TRB3 plasmids expressing WT-TRB3, D338A-TRB3, and ΔC20-TRB3. Cleavage of WT-TRB3 was observed in cells that were made apoptotic by treatment with tumor necrosis factor-α and cycloheximide (TNFα/CHX) (HeLa cells) or anti-Fas antibody (Jurkat cells), and this process was blocked by z-VAD-FMK, a caspase inhibitor (Figure 1D). As a result of *in vitro* experiment, the cleavage fragment derived from D338A-TRB3 and ΔC20-TRB3 was not detected in the apoptotic cells. Although the reduction of TRB3 levels was observed upon TNFα/CHX treatment, it may be due to proteasomal degradation and the rescue of protein levels seems to be the unexpected effect of z-VAD-FMK [21,22]. However, it could not be denied that lack of ΔC20-TRB3 stability is

caused by the deletion. Taken together, these results suggested that TRB3 was cleaved at Asp338 by caspases during apoptosis.

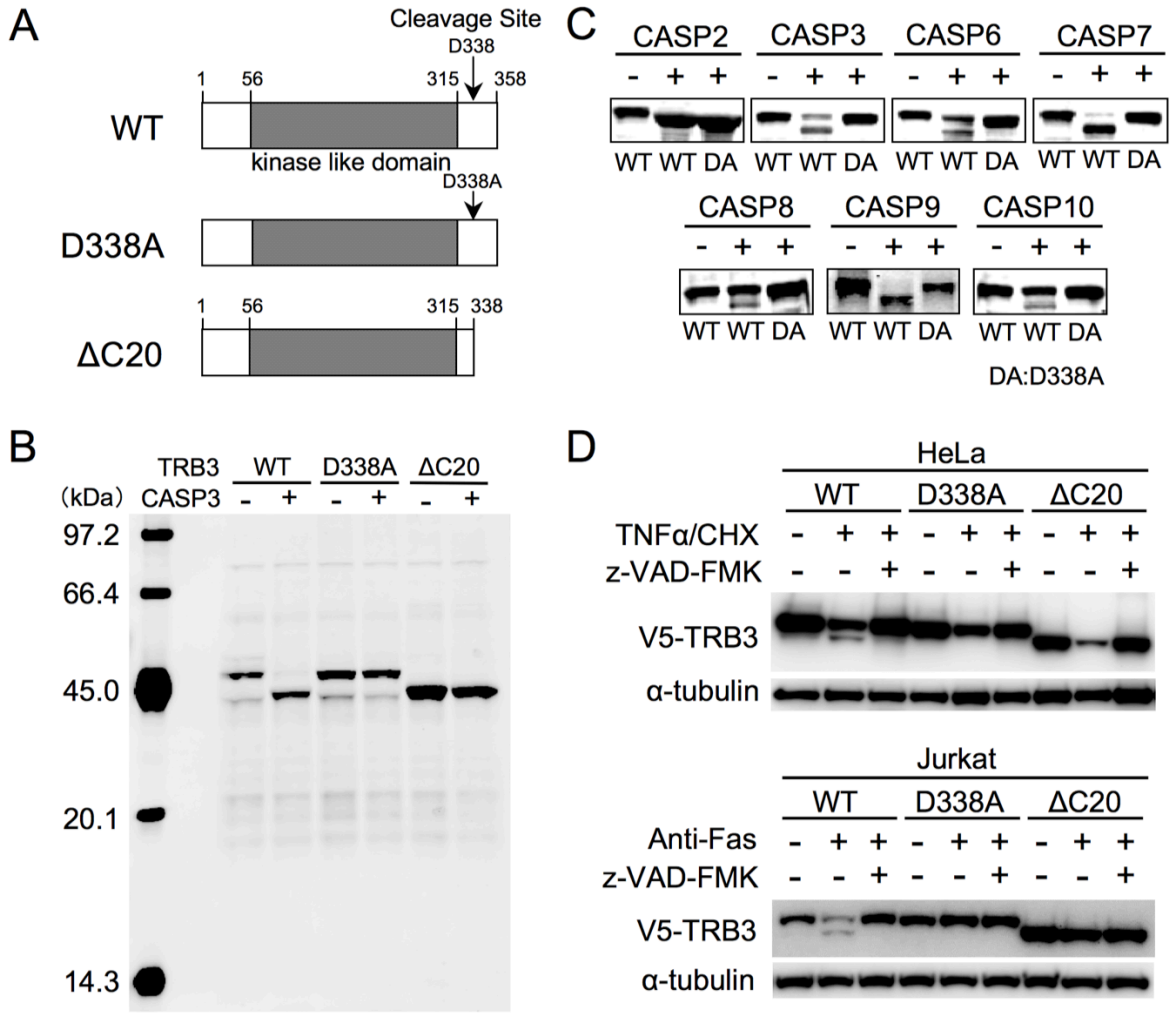

Figure 1. TRB3 is cleaved by caspases in vitro and in the apoptotic process. (A) Schematic representation of proteins expressed by the recombinant TRB3 constructs used in this study. WT, wild type TRB3; D338A, CASP3 cleavage-site mutant TRB3; and ΔC20, CASP3-cleaved form of TRB3. (B and C) Each recombinant TRB3 was synthesized and biotinylated using the wheat cell-free expression system as described in the Materials and Methods. The translation mixture was incubated with or without the indicated active caspase for 2 hr at 30°C. For the detection of N-terminal biotinylated-TRB3, the blot was probed with Alexa 488-conjugated streptavidin. DA denotes D338A-TRB3. (D) Twenty-four hours after transfection of HeLa and Jurkat cells with the indicated V5-tagged TRB3 expression plasmid, cells were treated with TNFα (20 ng/mL) /CHX (100 μM) (HeLa cells) or anti-Fas antibody (125 ng/mL) (Jurkat cells) in the absence or presence of z-VAD-FMK (100 μM) for 4 hr. DMSO was used as a treatment control. The cell lysates were subjected to immunoblot analysis using anti-V5 antibody to detect the N-terminal V5-tagged TRB3. α-Tubulin was used as an internal control.

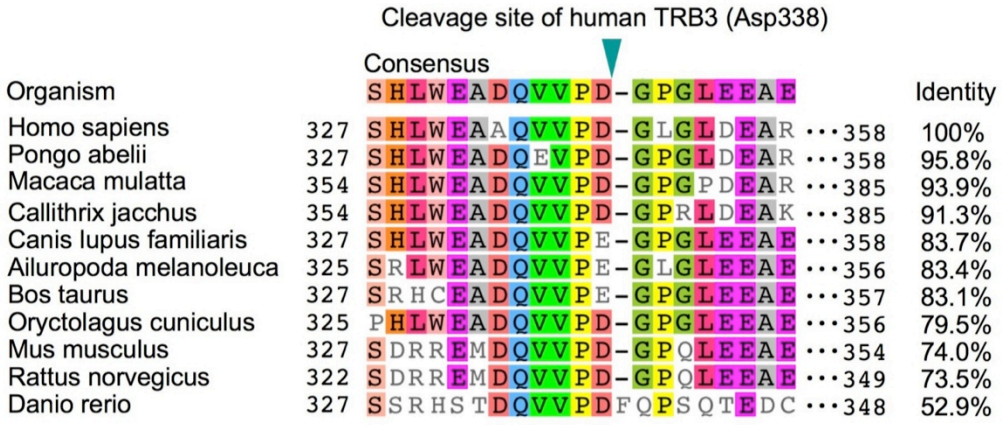

Figure S1 Sequence alignment analysis of TRB3 homologs. Organisms, more than 50% amino acid identity to human TRB3, were selected in this analysis. The result showed that TRB3 caspase-cleavage site is highly conserved. Although, homology of *Danio rerio* TRB3 is relatively low (52.9%), it should be noted that the P4-P1 substrate recognition motif (VVPD) is completely conserved. This raises a possibility that TRB3 is cleaved in various species and the cleavage has biological significance. Sequence alignment was carried out using the Geneious software.

Organism, Accession number: Homo sapiens, AAH27484; Pongo abelii, XP_002830205; Macaca mulatta, XP_002798226; Callithrix jacchus, XP_002747457; Canis lupus familiaris, XP_542943; Ailuropoda melanoleuca, XP_002925440; Bos taurus, NP_001069571; Oryctolagus cuniculus, XP_002710903; Mus musculus, NP_780302; Rattus norvegicus, NP_653356; Danio rerio, NP_998034

3.2. Cleavage of TRB3 promotes apoptosis along with CASP3 activation

TRB3 has been shown to be involved in the regulation of apoptosis under stress conditions. For example, overexpression of TRB3 under ER stress conditions produced pro-apoptotic effect [6]. Exact contribution of TRB3 to apoptosis, however, remains unclear at present. To determine how TRB3 cleavage affects apoptosis, I transiently overexpressed the cleavable TRB3 (WT) and non-cleavable TRB3 (D338A) in HeLa and Jurkat cells. Accordingly, both cells were separately transfected with the recombinant plasmids expressing WT-TRB3 or D338A-TRB3, or with the pcDNA3.1 empty vector (control vector), transfected cells were then treated with TNFα/CHX (HeLa cells) or anti-Fas antibody (Jurkat cells) to induce apoptosis and subsequently dead cells were counted. As shown in Figure 1D, expression levels of WT-TRB3 and D338A-TRB3 in both cells were very similar. Interestingly, the percentage of dead cells was higher in the WT-TRB3 expressing cells, but not in the D338A-TRB3 expressing cells, as compared to that in the control cells (Figure 2A and B). In both cells, the reagent-induced cell death was rescued back to the untreated control level when the stimuli were performed in the presence of the caspase inhibitor z-VAD-FMK (Figure S2), suggesting that cell death was due to apoptosis. These results suggest that the pro-apoptotic effect of TRB3 depends on its cleavage by caspases.

It is possible that the cleavage of TRB3 is an important event in the pro-apoptotic process. Because CASP3 activation is a critical step in the execution of apoptosis, I next investigated the effect of TRB3 cleavage on CASP3 activation. I used a luminescence-based assay to measure the CASP3/7 activity in cells. As shown, the CASP3/7 activity was found to be higher in the WT-TRB3 expressing cells, but not in the D338A-TRB3 expressing cells, than that in the control cells (Figure 2C and D). Taken together, these results suggest that cleavage of TRB3 is required for inducing further activation of CASP3 and/or CASP7, and in turn might promote apoptosis.

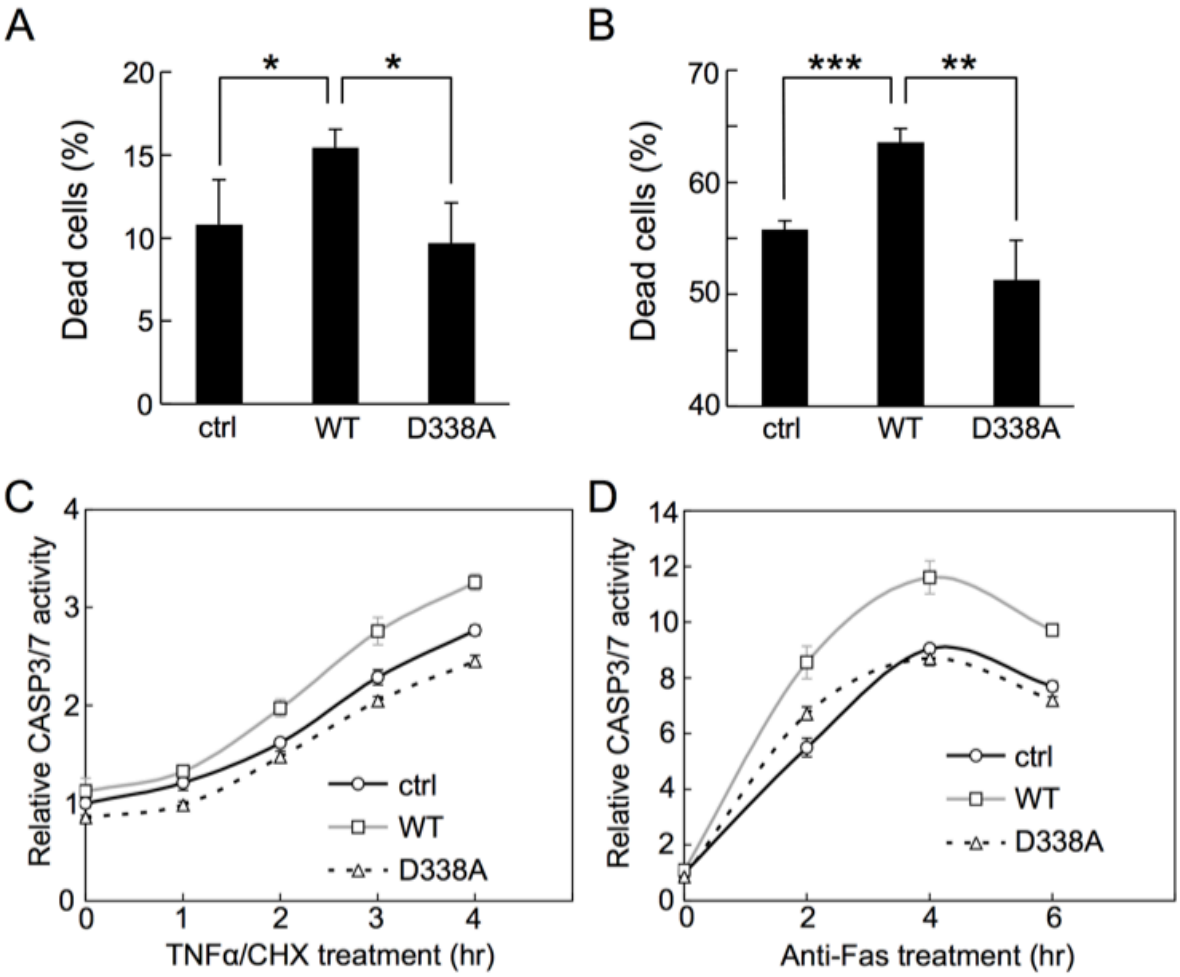

Figure 2. Cleavage of TRB3 promotes apoptosis along with CASP3 activation. (A and B) Twenty-four hours after transfection of HeLa (A) and Jurkat (B) cells with the indicated V5-TRB3 expression plasmid or control (ctrl) vector, the cells were treated with TNFα/CHX for 4 hr (HeLa cells) or anti-Fas antibody for 6 hr (Jurkat cells). The resulting dead cells were counted by trypan blue staining. Error bars indicate mean ± SD of three independent experiments. *P<0.05, **P<0.005, *** P<0.001, statistically significant difference. (C and D) Twenty-four hours after transfection with the indicated V5-TRB3 expression plasmid or control vector, HeLa (C) and Jurkat (D) cells were reseeded in 96-well plates (1.0×10^4 cells/well), and then treated with TNFα/CHX and anti-Fas antibody, respectively, for the indicated times and CASP3/7 activity was then measured using the luminometric Caspase-Glo® 3/7 Assay Kit. Each data point represents mean ± SD of three independent experiments.

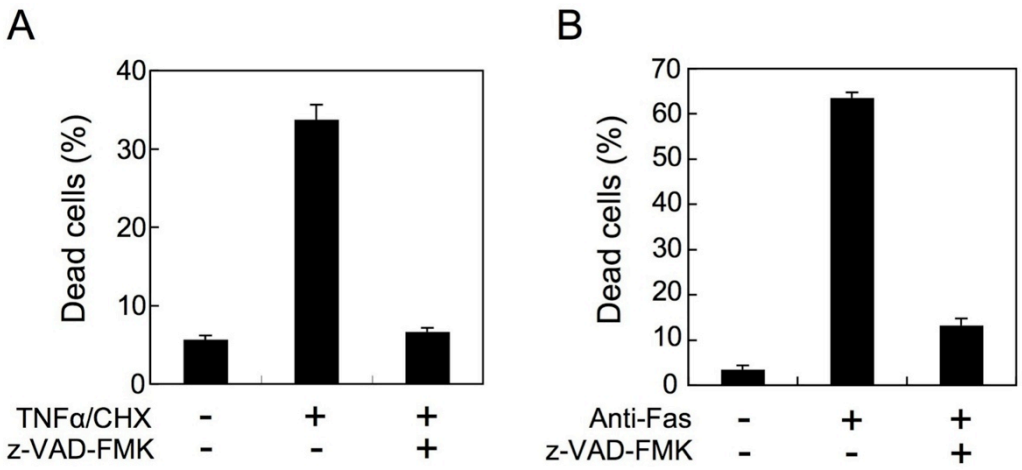

Figure S2 TNFα/CHX- and anti-Fas antibody-induced cell death was strongly inhibited by the caspase inhibitor z-VAD-FMK. (A, B) Twenty-four hours after transfection with the V5-WT-TRB3 expression plasmid, HeLa (A) and Jurkat (B) cells were treated with TNFα (20 ng/mL) /CHX (100 μM) for 4 hr and anti-Fas antibody (125 ng/mL) for 6 hr, respectively, in the absence or presence of z-VAD-FMK (100 μM). The resulting dead cells were counted by trypan blue staining. Error bars indicate mean ± SD of three independent experiments.

3.3. TRB3 inhibits CASP3 activation and subsequent apoptosis under ER stress condition

Tunicamycin treatment, which causes ER stress in cells, has been shown to induce TRB3 expression in several cell lines [6,16]. TRB3 expression was indeed induced in HeLa cells treated with 5 μM tunicamycin for 8 hours (Figure 3A), and the disappearance of endogenous TRB3 was clearly observed in apoptotic cells, although cleaved fragment was not observed due to use of C-terminus recognition antibody. Other antibodies could not also detect the cleaved fragment (Figure S3). Therefore, I next used tunicamycin treatment to examine how TRB3 cleavage affects CASP3/7 activation and subsequent apoptosis under ER stress conditions. D338A-TRB3 expressing cells were resistant to CASP3/7 activation and death (Figure 3B and C). Surprisingly, I also observed anti-apoptotic effect, rather than pro-apoptotic effect, in WT-TRB3 expressing cells, although this anti-apoptotic effect was lower than that in D338A-TRB3 expressing cells (Figure 3B and C). As previously reported [6], a major portion of the tunicamycin-induced cell death also appears to be apoptotic cell death, because cell death was strongly inhibited in the presence of z-VAD-FMK (Figure S4). Unlike in the case of TNFα/CHX- or anti-Fas antibody-induced apoptosis (as shown in Figure 2), WT-TRB3 actually rescued cells from death under ER stress condition. To explain this result, I examined the cleavage of WT-TRB3 during ER stress. I found hardly any cleavage of WT-TRB3 in tunicamycin-treated cells (Figure 3D), although it was clearly seen in TNFα/CHX- and anti-Fas antibody-treated cells (Figure 1D and 3D). Most of the subsequent reduction of WT-TRB3 after tunicamycin treatment may be not resulting consequence by cleavage because TRB3 is rapidly degraded through the ubiquitin-proteasome pathway as previously described [22] and non-cleavable TRB3 (D338A) was also reduced in a similar manner. Moreover, ER stress regulates protein synthesis via the unfolded protein response (UPR). Therefore, the global reduction of protein levels could be caused by ER stress condition itself. Next, to clarify the observed difference in susceptibility to cleavage, I measured the CASP3/7 activity in TNFα/CHX- or tunicamycin-treated cells. The increase in CASP3/7 activity was very slow during the tunicamycin-induced ER stress, and was significantly lower than in cells undergoing apoptosis induced by TNFα/CHX treatment (Figure 3E). This result suggests that the ER

stress-induced CASP3/7 activity, at least in this condition, is not so high as to actively cleave TRB3.

To assess whether TRB3 itself is required for the modulation of CASP3/7 activation, I used siRNA to knockdown the TRB3 expression in cells under ER stress condition (Figure 3F). As shown, TRB3 siRNA (siTRB3) specifically reduced the expression of endogenous TRB3 upto 24 hours following the tunicamycin treatment (Figure 3G), by which time the relative activity of CASP3/7 increased over the activity found in negative control siRNA (siNC)-transfected cells (Figure 3H). Taken together, these results strongly suggest that TRB3 intrinsically blocks CASP3 and/or CASP7 activation and subsequent apoptosis under TRB3 non-cleavable conditions, such as ER stress.

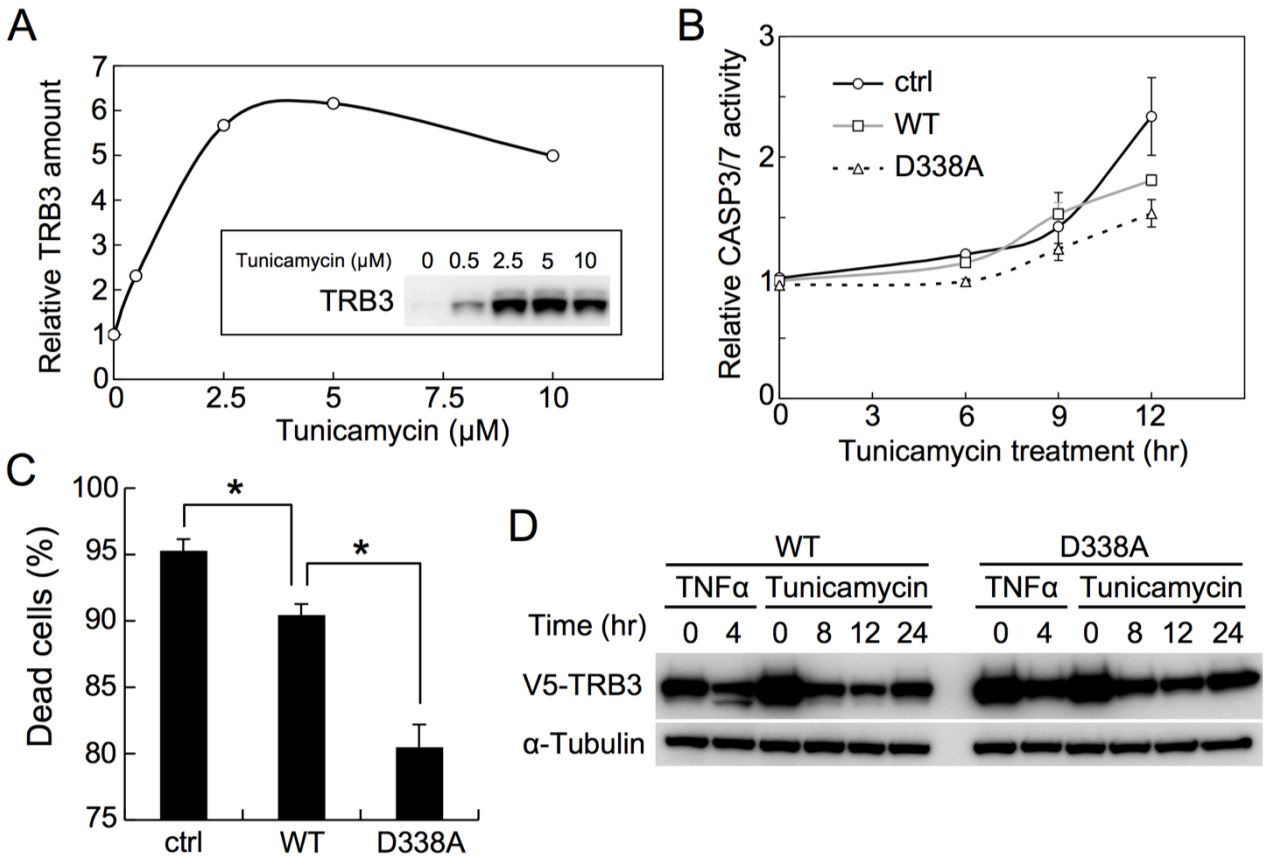

Figure 3. TRB3 inhibits CASP3 activation and subsequent apoptosis under ER stress condition. (A) HeLa cells were treated with the indicated concentrations of tunicamycin for 8 hr. The effective concentration of tunicamycin needed for inducing TRB3 expression was determined by densitometric image analysis. (B) CASP3/7 activity in HeLa cells was measured as described in the legend of Figure 2C, except that here apoptosis was induced by incubation with 5 μM tunicamycin for the indicated times. Each data point represents mean ± SD of three independent experiments. (C) Twenty-four hours after transfection with the indicated V5-TRB3 expression plasmid or control vector, HeLa cells were treated with tunicamycin for 48 hr. The resulting dead cells were counted by trypan blue staining. Error bars indicate mean ± SD of four independent experiments. *P<0.001. (D) Twenty-four hours after transfection with the given V5-TRB3 expression plasmid, HeLa cells were treated with TNFα/CHX or tunicamycin for the indicated times. The cell lysates were subjected to immunoblot analysis using the anti-V5 antibody. α-Tubulin was used as an internal control.

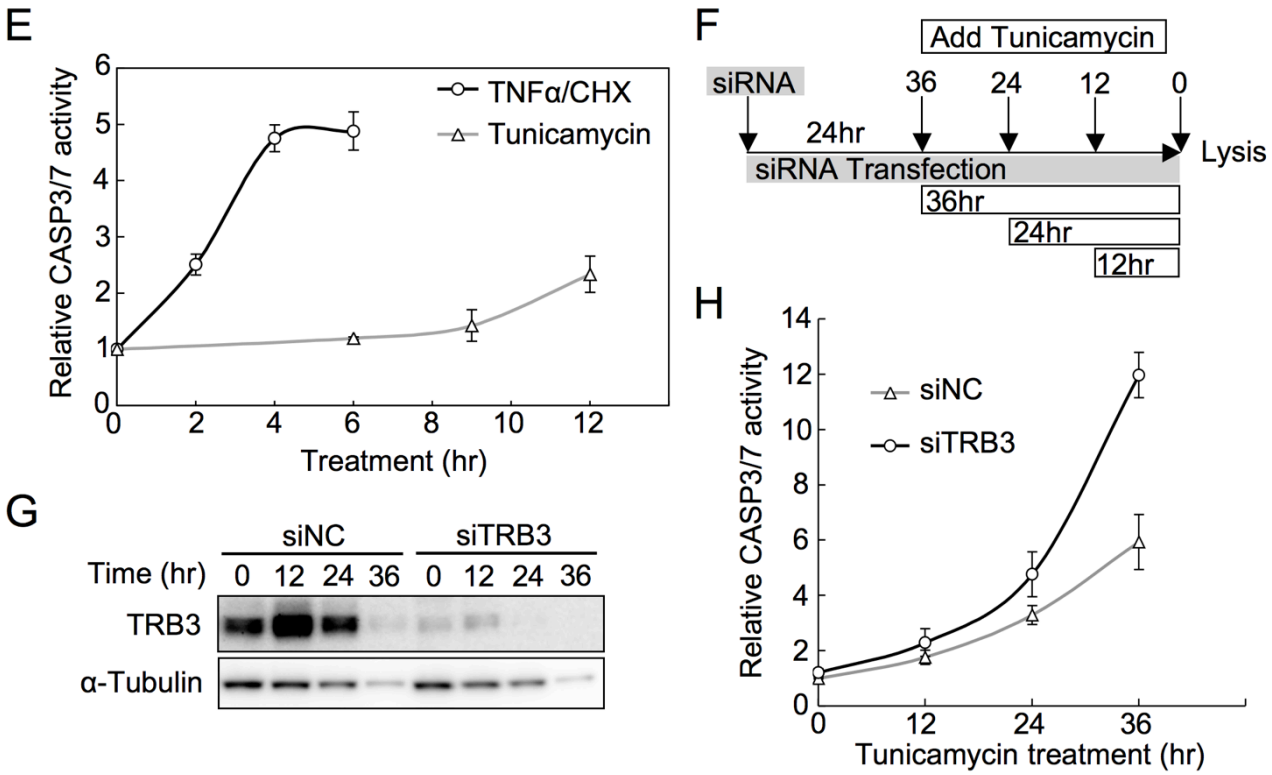

Figure 3. TRB3 inhibits CASP3 activation and subsequent apoptosis under ER stress condition. (E) HeLa cells plated in 96-well plates (1.0×10^4 cells/well) were treated with TNFα/CHX or tunicamycin for the indicated times. CASP3/7 activity was measured using the luminometric Caspase-Glo® 3/7 Assay Kit. Each data point represents mean ± SD of three independent experiments. (F-H) HeLa cells were transfected with negative control siRNA (siNC) or TRB3 siRNA (siTRB3). Twenty-four hours after, the cells were treated with tunicamycin for the indicated time points (F). The cell lysates were subjected to immunoblot analysis using the anti-TRB3 antibody (G). Cell lysates were also used for the Caspase-Glo® 3/7 assay to measure the CASP3/7 activity (H). The relative CASP3/7 activity was then determined after normalizing each value with respect to the relative amount of expressed α-Tubulin as estimated by densitometric image analysis. Each data point represents mean ± SD of three independent experiments.

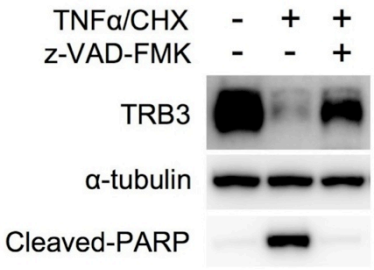

Figure S3 Cleavage of endogenous TRB3 in apoptotic cells. HeLa cells were treated with tunicamycin (5 μM) for 8 hr, and then treated with TNFα/CHX in the absence or presence of z-VAD-FMK (100 μM) for 3 hr. DMSO was used as a treatment control. The cell lysates were subjected to immunoblot analysis using anti-TRB3 antibody. Cleaved PARP (#9541, Cell Signaling Technology) is a marker of apoptosis. α-Tubulin was used as an internal control.

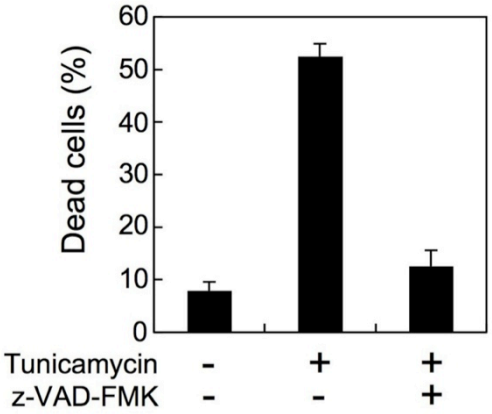

Figure S4 Tunicamycin-induced cell death was strongly inhibited by the caspase inhibitor z-VAD-FMK. Twenty-four hours after transfection with the control vector, HeLa cells were treated with tunicamycin for 36 hr in the absence or presence of z-VAD-FMK. The resulting dead cells were counted by trypan blue staining. Error bars indicate mean ± SD of three independent experiments.

3.4. TRB3 expression induces nuclear translocation of proCASP3

In Figure 3, I have presented evidence that suggests that TRB3 negatively regulates the activation of CASP3. However, the premature CASP3 (i.e. procaspase-3; proCASP3) and TRB3 are differently localized in cells; proCASP3 is predominantly localized in the cytoplasm [23,24], whereas TRB3 is localized in the nucleus [5,7]. Thus, even though TRB3 is a substrate for CASP3, how these two molecules would interact with each other still remains elusive. To gain further insights about that, I next examined whether the subcellular localization of proCASP3 would be affected by TRB3 expression. For this purpose, I constructed a recombinant plasmid expressing an EmGFP-tagged inactive proCASP3 mutant (C163S-proCASP3-EmGFP), in which the active site cysteine residue was altered to a serine residue (C163S) to prevent apoptosis. I next cotransfected HeLa cells with the C163S-proCASP3-EmGFP and WT-TRB3 expression plasmids, and subsequently assessed the subcellular localization based on the relative fluorescence intensity of EmGFP by using confocal microscopy. Under normal culture condition, C163S-proCASP3-EmGFP predominantly exhibited cytoplasmic localization (left panels in Figure 4A and B, see arrowheads), which is consistent with the known localization of proCASP3. Interestingly, C163S-proCASP3-EmGFP was found mainly in the nucleus of cells coexpressing WT-TRB3 (Figure 4A, see arrow).

As shown in Figure 3A, under normal culture condition cells maintained the endogenous TRB3 expression at a relatively low level, which significantly increased after tunicamycin treatment for 8 hours. So next, I examined the localization of C163S-proCASP3-EmGFP under tunicamycin-induced ER stress condition. Because active CASP3 was hardly detected by immunofluorescence in tunicamycin-treated morphologically normal cells (98.7% were active CASP3 negative; 100 cells were assessed in three independent experiments), I assumed that C163S-proCASP3-EmGFP as the premature form (i.e. proCASP3) in these cells (Figure S5). Increased amount of C163S-proCASP3-EmGFP was found in the nucleus of tunicamycin-treated cells (Figure 4B right panel, see arrowheads). Furthermore, I could monitor the nuclear accumulation of C163S-proCASP3-EmGFP by live imaging of cells up to 24 hours following the tunicamycin treatment (Figure 4C). The number of cells expressing nuclear

C163S-proCASP3-EmGFP was increased by tunicamycin treatment and also by coexpression of WT-TRB3 (Figure 4D). The difference in the cytoplasmic/nuclear ratio of C163S-proCASP3-EmGFP between the tunicamycin-treated and WT-TRB3-overexpressed cells suggests that the nuclear translocation efficiency of C163S-proCASP3-EmGFP might be dependent on the TRB3 expression level. A similar phenotype was observed in D338A-TRB3 expressing cells (Figure S6).

Using cells expressing HA-tagged inactive proCASP3 mutant (C163S-proCASP3-HA), I also obtained similar results of the localization before and after tunicamycin treatment (Figure S7). Therefore, I further examined whether the efficiency of nuclear translocation of C163S-proCASP3-HA would decrease by microRNA (miRNA)-mediated down-regulation of endogenous TRB3 expression. To this end, I designed two types of artificial miRNA targeting TRB3 mRNA (miR-TRB3-CDS and miR-TRB3-3'UTR), and which specifically suppressed endogenous TRB3 expression (Figure S8). I could identify the miRNA expressing cells by cocistronic expression of EmGFP from the same plasmid. The localization of C163S-proCASP3-HA was assessed in EmGFP expressing cells (Figure 4E and F). Consequently, the phenotype of cells positive for nuclear C163S-proCASP3-HA was decreased in miR-TRB3 expressing cells under tunicamycin-induced ER stress condition. Taken together, these results suggest that ER stress induced TRB3 expression leads to nuclear translocation of proCASP3.

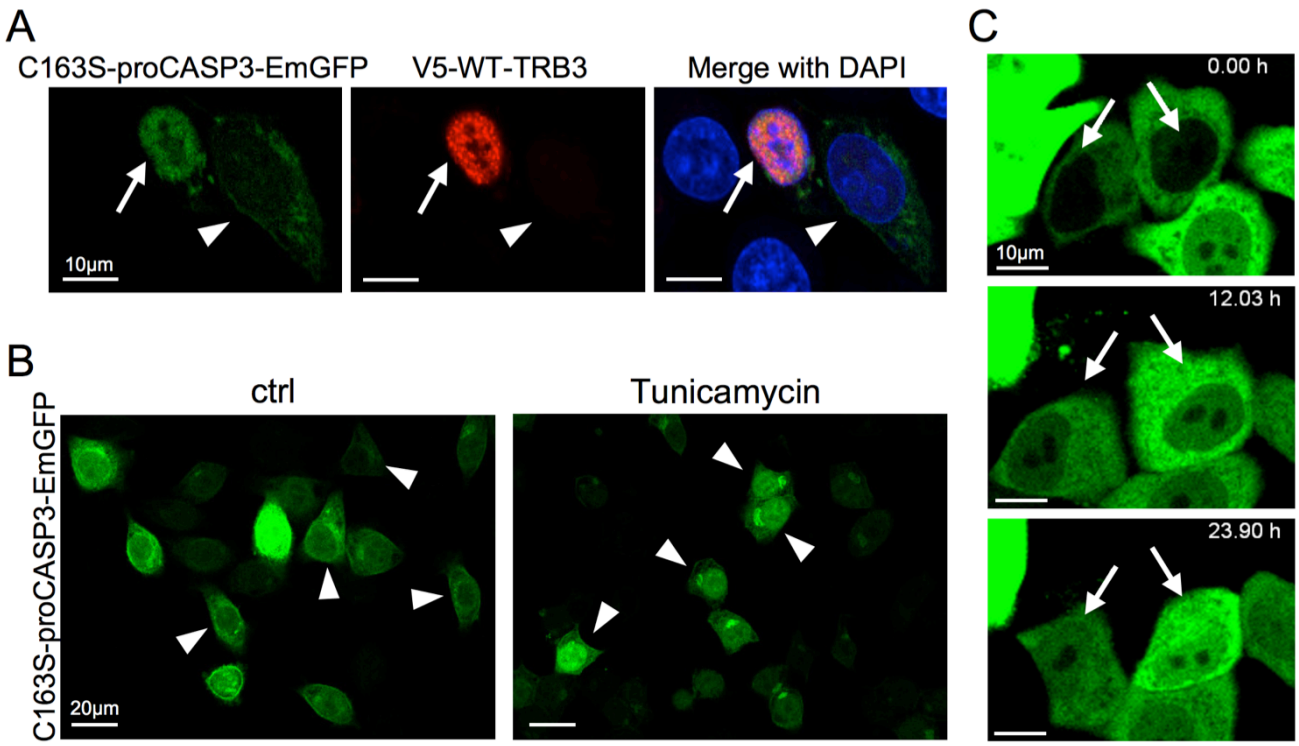

Figure 4. TRB3 expression induces nuclear translocation of proCASP3. (A) HeLa cells were cotransfected with the C163S-proCASP3-EmGFP and V5-WT-TRB3 expression plasmids. After 24 hr, the cells were stained with anti-V5 antibody (red) and counterstained with DAPI (blue). Arrow and arrowhead indicated V5-WT-TRB3 positive and negative cells respectively. Scale bars = 10 μm. (B) Twenty-four hours after transfection with the C163S-proCASP3-EmGFP expression plasmid, HeLa cells were incubated with or without tunicamycin for 8 hr. Arrowheads showed representative phenotypes of C163S-proCASP3-EmGFP localization in each condition. Scale bars = 20 μm. (C) Twenty-four hours after transfection with the C163S-proCASP3-EmGFP expression plasmid, HeLa cells were treated with tunicamycin, and localization of C163S-proCASP3-EmGFP was simultaneously monitored for 24 hr by live imaging. Representative frames displaying scenes of nuclear translocation (arrows) are shown. Scale bars = 10 μm.

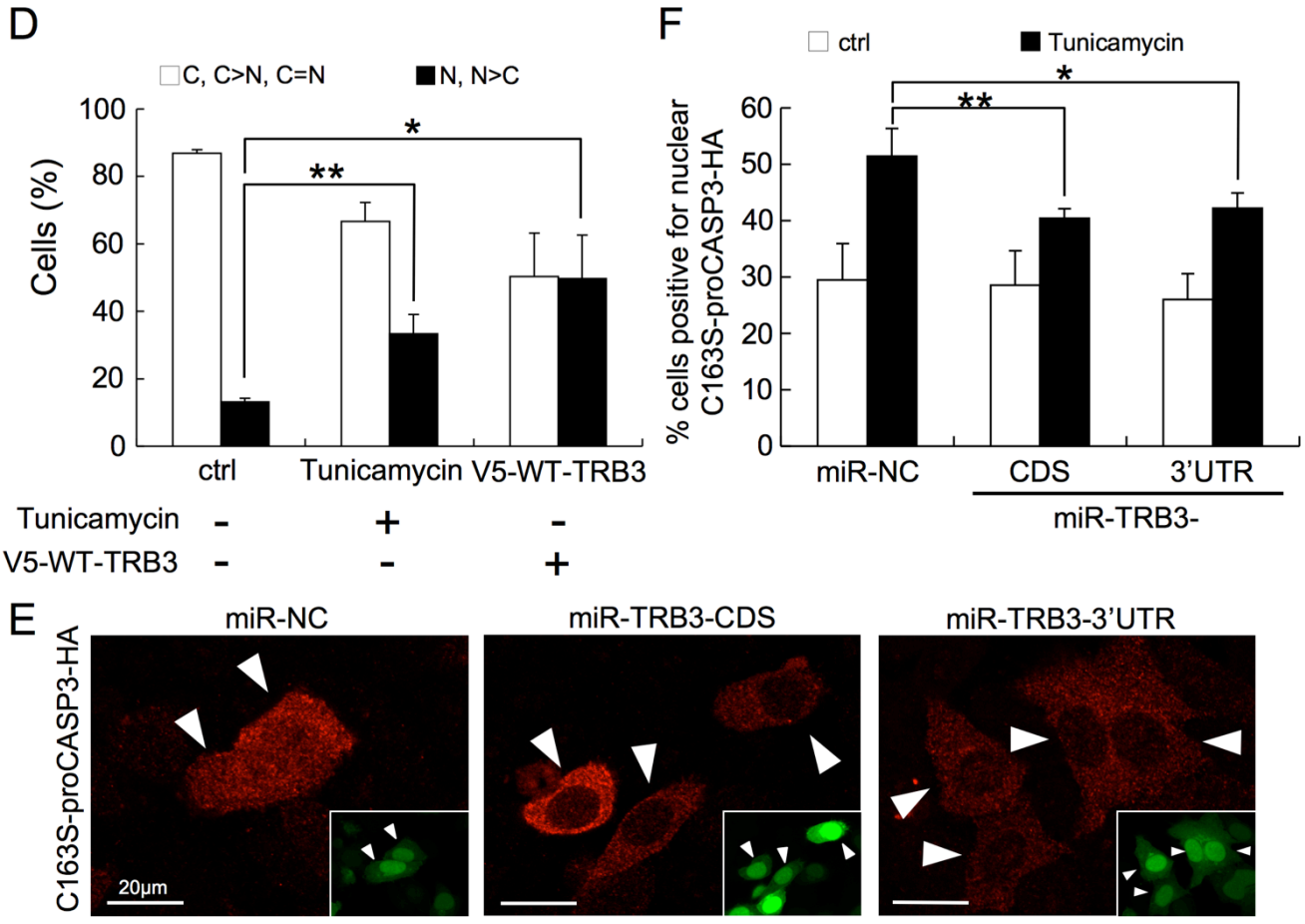

Figure 4. TRB3 expression induces nuclear translocation of proCASP3. (D) Localization of C163S-proCASP3-EmGFP was quantified as cytoplasmic, mainly cytoplasmic or cytoplasmic equal to nuclear (C, C>N, C=N), or as nuclear or mainly nuclear (N, N>C) under conditions described above (Figure 4A, V5-WT-TRB3; Figure 4B, ctrl or Tunicamycin). This localization was also assessed in cells coexpressing V5-WT-TRB3 (right bar graph). Over 30 cells were assessed in three independent experiments. Error bar: mean ± SD. *P<0.01, **P<0.005. (E) HeLa cells were cotransfected with the C163S-proCASP3-HA and indicated artificial miRNA expression plasmids. After 24 hr, the cells were incubated with tunicamycin for 8 hr. The localization of C163S-proCASP3-HA was observed by immunofluorescence staining with an anti-HA antibody (red). The miRNA expressing cells of inner panel were visualized by cocistronic expression of EmGFP. Arrowheads showed the C163S-proCASP3-HA expressing cells. Scale bars = 20 μm. (F) The cells positive for nuclear C163S-proCASP3-HA (N, N>C, N=C) were quantified by immunofluorescence staining with an anti-HA antibody. Over 30 cells positive for EmGFP were assessed in six independent experiments. Error bar: mean ± SD. *P<0.005, ** P<0.001. miR-NC denotes negative control miRNA.

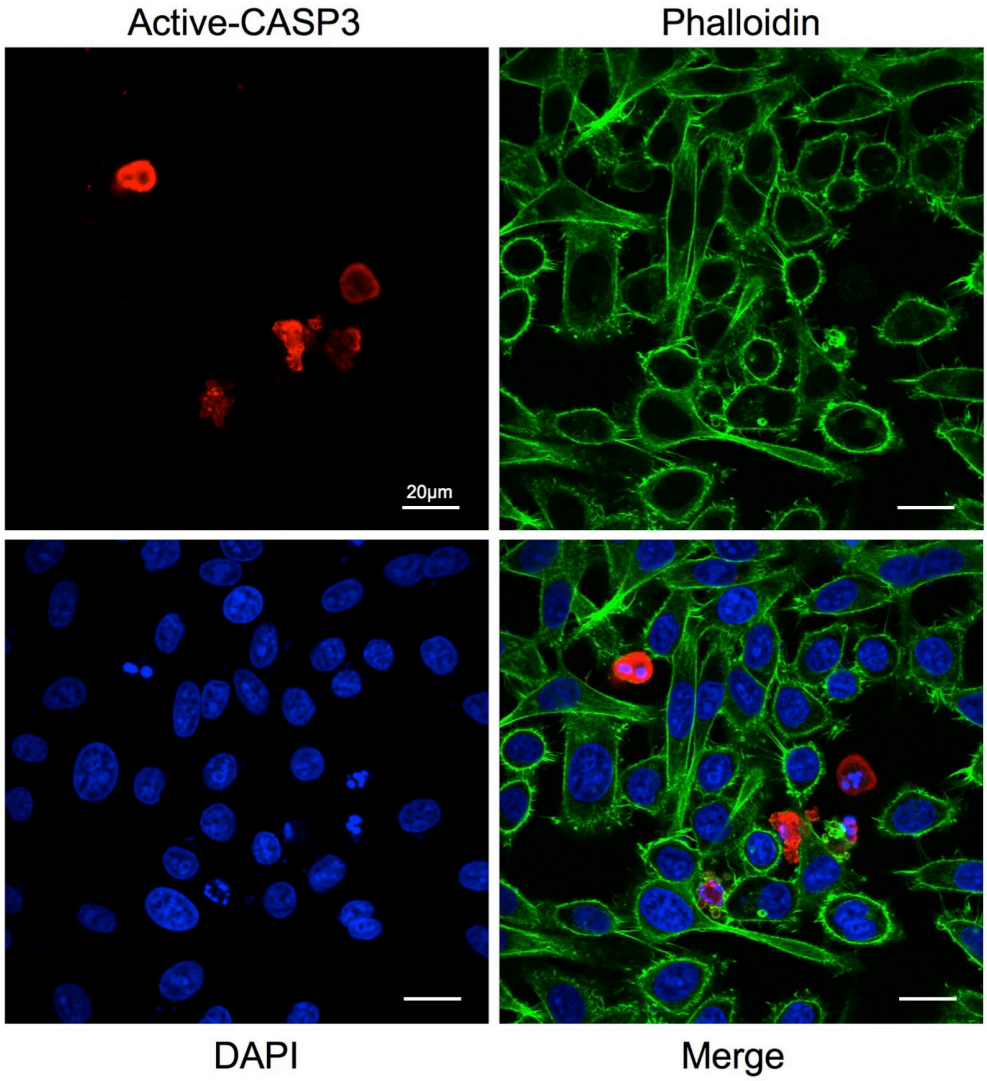

Figure S5 Active CASP3 was hardly detected in tunicamycin-treated morphologically normal cells. HeLa cells grown on coverslips were treated with tunicamycin for 8 hr. The fixed cells were stained with anti-Active-CASP3 antibody (red), and counterstained with DAPI (blue) and Alexa 488-conjugated phalloidin (green) to visualize the nuclei and cell morphology, respectively. 100 cells were assessed in three independent experiments, and 98.7% of tunicamycin-treated morphologically normal cells were active CASP3 negative. Scale bars = 20 μm.

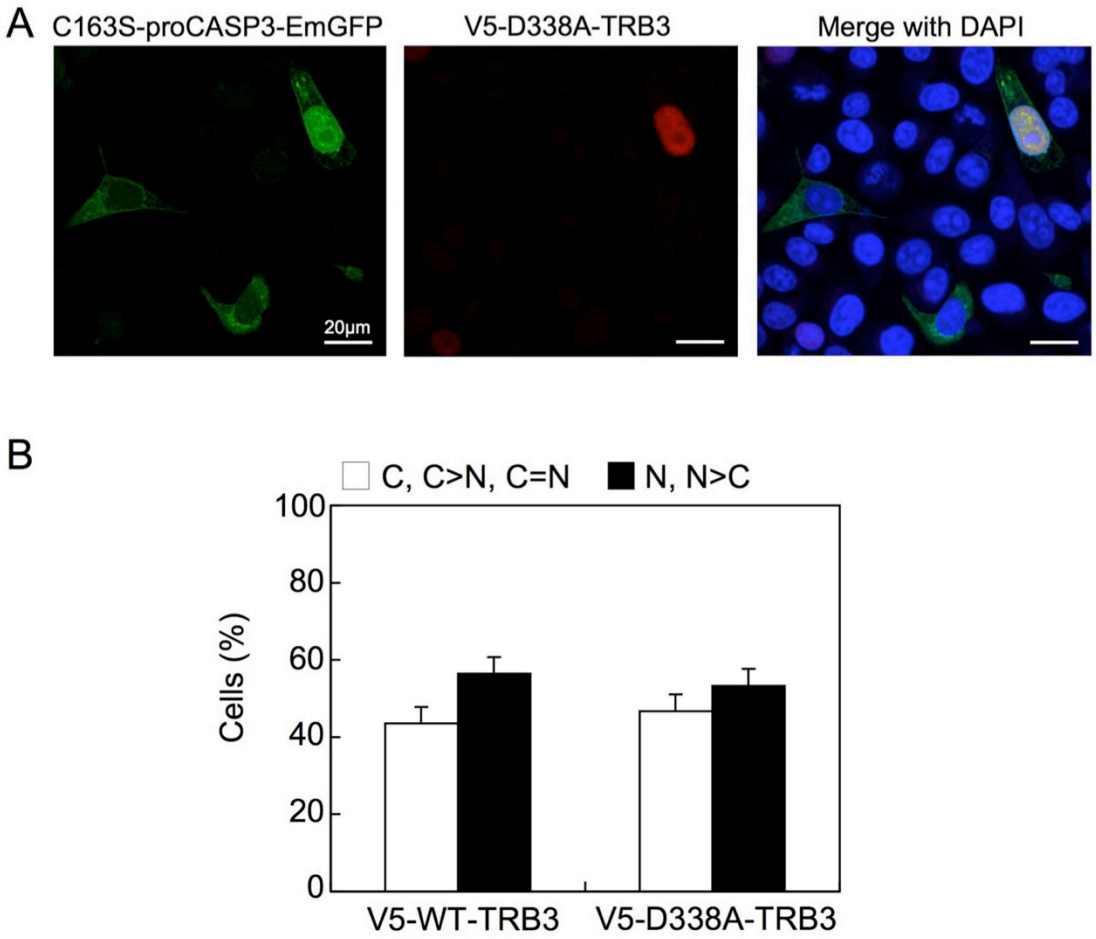

Figure S6 Nuclear translocation efficiency of proCASP3 mediated by D338A-TRB3 was almost same as that by WT-TRB3. (A) HeLa cells grown on coverslips were cotransfected with the EmGFP-tagged inactive proCASP3 mutant (C163S-proCASP3-EmGFP) and V5-D338A-TRB3 expression plasmids, and then incubated for 24 hr. The fixed cells were stained with anti-V5 antibody (red) and counterstained with DAPI (blue) to visualize the nuclei. Scale bars = 20 μm. (B) Twenty-four hours after transfection, HeLa cells grown on coverslips were fixed, and then stained as described above. Localization of C163S-proCASP3-EmGFP in cells that are also expressing TRB3 from the respective plasmid was quantified as cytoplasmic, mainly cytoplasmic or cytoplasmic equal to nuclear (C, C>N, C=N), or as nuclear or mainly nuclear (N, N>C). Over 30 cells were assessed in three independent experiments. Error bar: mean ± SD.

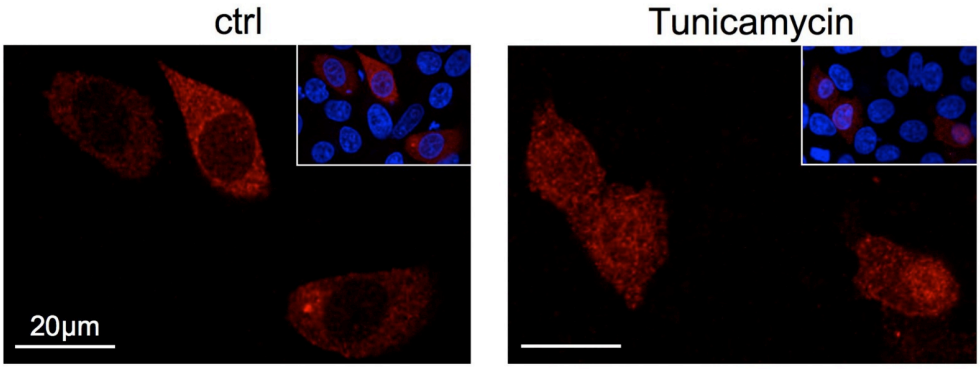

Figure S7 The localization of C163S-proCASP3-HA. HeLa cells grown on coverslips were transfected with the C163S-proCASP3-HA expression plasmid. After 24 hr, the cells were incubated with or without tunicamycin for 8 hr. The localization of C163S-proCASP3-HA was observed by immunofluorescence staining with an anti-HA antibody (red). Inner panel was merged with DAPI (blue) to visualize the nuclei. Scale bars = 20 μm.

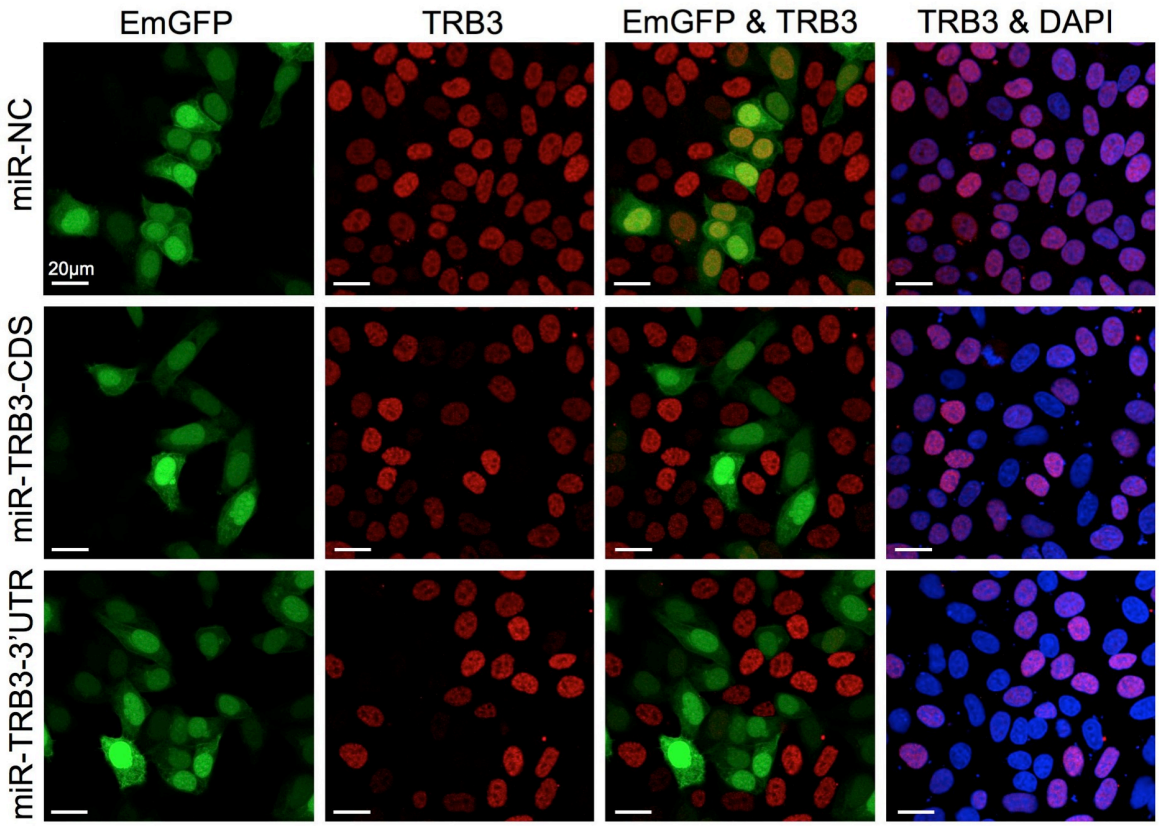

Figure S8 Artificial miRNAs targeting TRB3 mRNA specifically suppress endogenous TRB3 expression. HeLa cells grown on coverslips were transfected with the indicated artificial miRNA expression plasmid that enable identify the miRNA expressing cells by cocistronic expression of EmGFP. After 24 hr, the cells were treated with tunicamycin for 8 hr, and then fixed. Endogenous TRB3 and nuclei were visualized by immunofluorescence staining with an anti-TRB3 antibody (red) and DAPI (blue) respectively. Scale bars = 20 μm. miR-NC denotes negative control miRNA.

3.5. Nuclear proCASP3 did not promote apoptosis

Results shown in Figure 3 and 4 suggested that TRB3 expression produced anti-apoptotic effect and it also induced nuclear translocation of proCASP3 under ER stress condition. I hypothesized that inhibition of apoptosis by TRB3 resulted from the nuclear translocation of proCASP3. Paradoxically speaking, the presence of proCASP3 in the cytoplasm, but not that in the nucleus, appears to be more important for the execution of apoptosis, because it has been proposed that the activation of CASP3 initially occurs in the cytoplasm, and the activated CASP3 then gets translocated to the nucleus [25]. To validate my hypothesis, I constructed three recombinant plasmids – one expressing EmGFP-tagged wild type proCASP3 (proCASP3-EmGFP), the second expressing nuclear localization signal (NLS) containing proCASP3-EmGFP (proCASP3-NLS-EmGFP) and the third expressing DsRed-NLS fusion protein (DsRed-NLS; control), and used them to investigate the effect of forced nuclear expression of proCASP3 on apoptosis. Accordingly, HeLa cells were separately transfected with these plasmids, and then the transfected cells were plated together in one glass bottom dish. After inducing apoptosis, EmGFP-fusion protein positive and DsRed positive cells were observed by live imaging. As expected, under normal culture condition (i.e. cells not fixed), proCASP3-EmGFP was localized in the cytoplasm (Figure 5A left panel), whereas proCASP3-NLS-EmGFP (middle panel) and DsRed-NLS (right panel) were localized only in the cell nucleus. The anti-Fas antibody was used for apoptosis induction, because it did not induce nuclear translocation of proCASP3 at least during imaging. As shown in Figure 5B and C, apoptotic cell death, based on cell morphology, was preferentially induced in cells expressing the cytoplasmic proCASP3 (proCASP3-EmGFP) than in cells expressing the nuclear proCASP3 (proCASP3-NLS-EmGFP) or the nuclear DsRed-NLS (Figure 5D and see Movie S1). These results strongly suggest that nuclear distribution of proCASP3 is not critical for the execution of apoptosis. Taken together with the previous section, my results suggest that TRB3 expression prevents CASP3 activation by nuclear translocation of proCASP3, and thereby inhibits apoptosis.

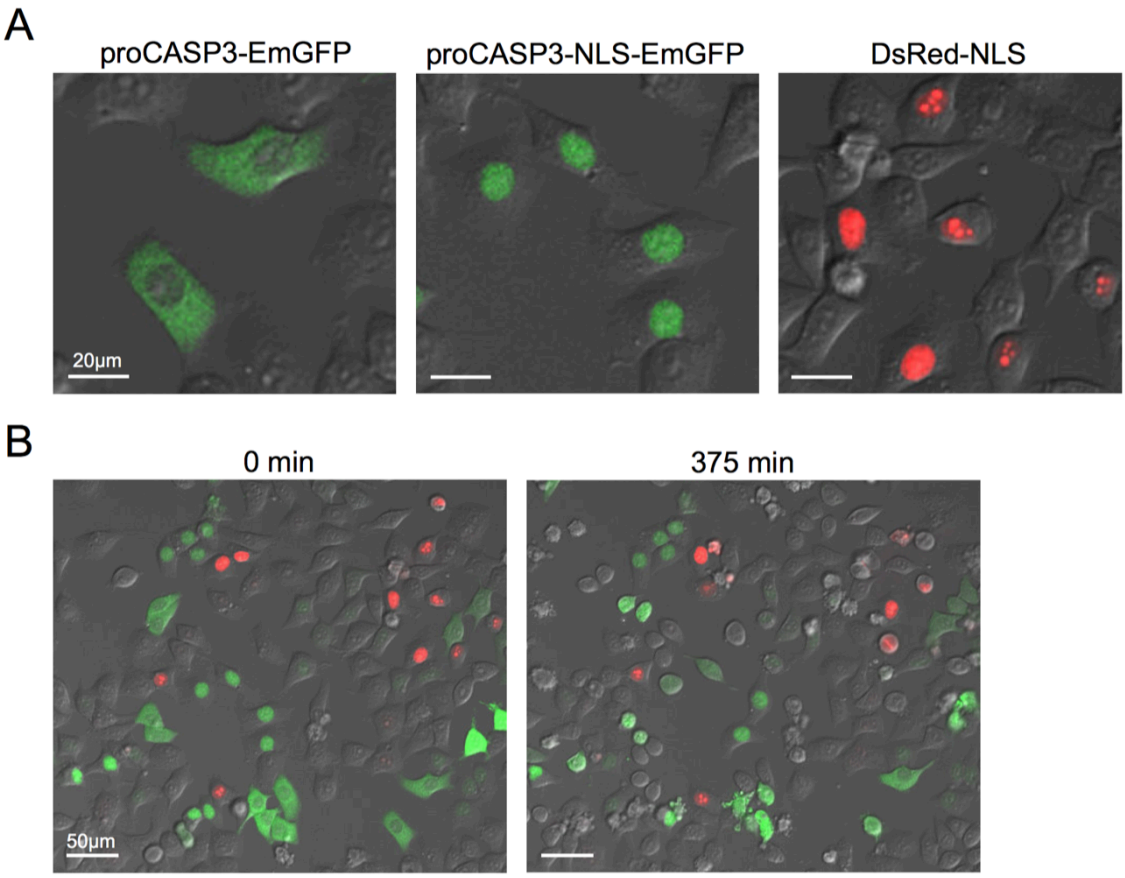

Figure 5. Nuclear proCASP3 did not promote apoptosis. (A-D) HeLa cells were separately transfected with the plasmid expressing EmGFP-tagged wild type proCASP3 (proCASP3-EmGFP), nuclear localization signal (NLS) containing proCASP3-EmGFP (proCASP3-NLS-EmGFP), or DsRed-NLS fusion protein (DsRed-NLS). After 24 hr, transfected cells were trypsinized and plated together in one glass bottom dish. After a further 24 hr, apoptosis was induced by the addition of anti-Fas antibody. Cells expressing the indicated fusion protein are shown (A). Behavior of the EmGFP-fusion protein positive and DsRed positive cells (same field at different times) was recorded by live imaging (B). Scale bars = 20 μm (A), 50 μm (B).

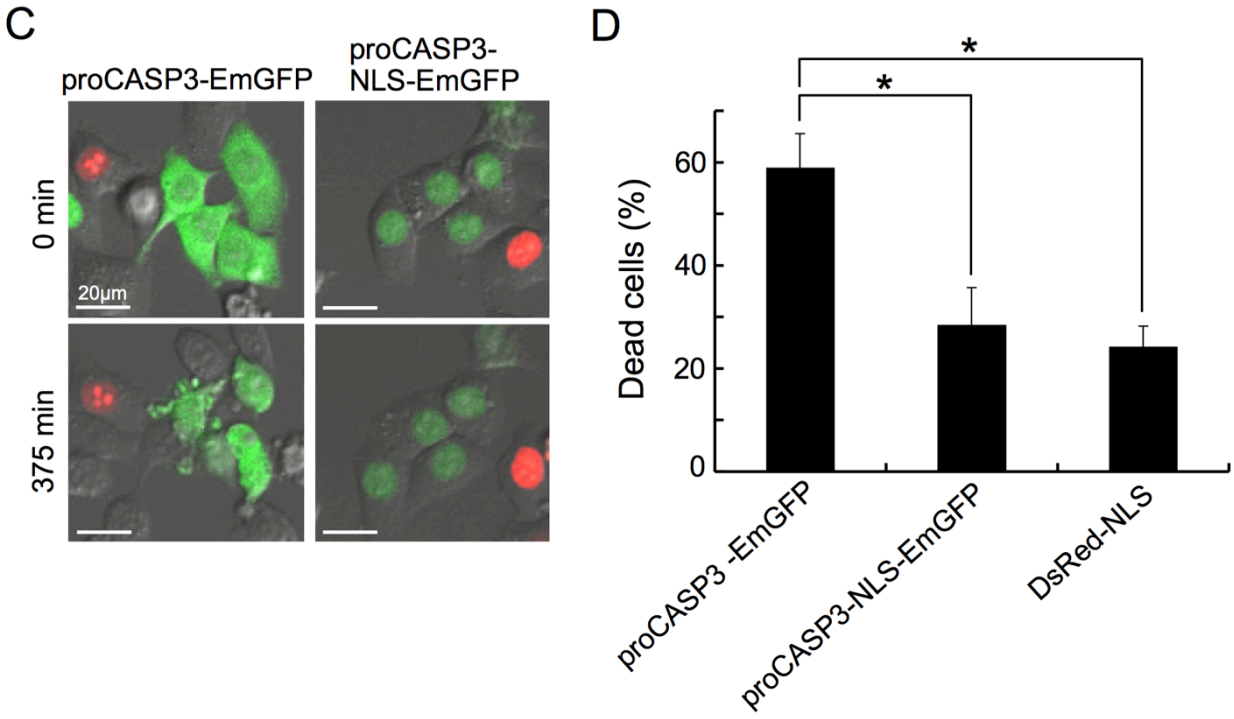

Figure 5. Nuclear proCASP3 did not promote apoptosis. (C) Representative frames showing images of cells expressing the indicated fusion protein in a given field, as recorded in Figure 5B, are displayed. Scale bars = 20 μm. (D) The number of apoptotic cells (based on cell morphology) was counted at 450 min after apoptosis induction by anti-Fas antibody. A minimum number of 30 cells were counted in a field for each type of fusion protein expressing cells. Four fields were randomly chosen for counting the number of apoptotic cells. Error bar: mean ± SD. *P<0.001.

4. DISCUSSION

TRB3 expression is up-regulated in a variety of cell types under various stress conditions including ER stress, nutrient deprivation, hypoxia and oxidative stress [1,6,17,26]. However, the exact role of TRB3 expression in stress response is controversial because it has been reported that the stress-induced expression of TRB3 exhibited both pro-apoptotic [6,16,27,28] and anti-apoptotic [17,26] effects. Several studies have led to the suggestion that the opposite behavior of TRB3 was due to its putative role as a stress sensor [6,13,29]. The exact molecular mechanism, however, remains unclear.

Recently, we found that TRB3 was cleaved by CASP3, and this observation could easily be correlated to the previous reports by suggesting that TRB3 is involved in the regulation of apoptosis. In this study, I further found that the C-terminal region of TRB3 was a target for most caspases (Figure 1C). In fact, the expressed TRB3 was cleaved within a few hours of inducing apoptosis using TNFα/CHX or anti-Fas antibody (Figure 1D and 3D). In this case, CASP3/7 activation and subsequent apoptosis were promoted in WT-TRB3 expressing cells, but the pro-apoptotic effect of TRB3 was not observed in cells expressing the non-cleavable D338A-TRB3 (Figure 2). Additionally, I have found that ΔC20-TRB3 (see Figure 1A), which could be produced by multiple caspases during the apoptotic process (Figure 1C and D), did not have any pro-apoptotic effect (Figure S9), suggesting that the pro-apoptotic effect is not mediated by the cleaved TRB3 (ΔC20) but likely requires the C-terminal region of TRB3 and/or the cleavage event to function. Indeed, a peptide, around 10 residues long, such as amyloid β-peptide, has been shown to induce apoptosis [30,31]. In contrast to the above case, TRB3 cleavage was hardly observed even if the cells were exposed to ER stress by tunicamycin for as long as 24 hours (Figure 3D). CASP2 has been shown to be involved in ER stress with treatment of high tunicamycin condition (> 20 μg/mL = 24 μM) [32,33] and has TRB3 cleavage ability (Figure 1C). However CASP2 activation may be not found in low tunicamycin condition (< 5 μg/mL = 6 μM) [32]. Actually, in my condition (5 μM) it was not detected (data not shown), and TRB3 cleavage was also hardly observed (Figure S10A), like Figure 3D. In addition, treatment of CASP2 inhibitor (z-VDVAD-FMK) rescued only small number of the

dead cells (Figure S10B). Therefore, at least in my condition, CASP2 seems to have only limited impact on apoptosis by tunicamycin. Interestingly, in these cases, CASP3/7 activation and subsequent apoptosis were slightly inhibited in WT-TRB3 expressing cells (Figure 3B, C and S10B), and the results shown in Figure 4 and 5 suggested that the anti-apoptotic effect was due to the TRB3-mediated nuclear translocation of proCASP3. The non-cleavable D338A-TRB3 was also localized in the nucleus (Figure S6A), and its translocation efficiency of proCASP3 was almost same as that by WT-TRB3 (Figure S6B). But, in the case of chronic stress, the anti-apoptotic effect of WT-TRB3 was lower than that of D338A-TRB3 (Figure 3B and C), likely as a result of the combined pro-apoptotic effect of the cleavable TRB3 (i.e. WT-TRB3). To investigate how TRB3 affects apoptosis induced by intrinsic stimulus independent of ER stress, I further used staurosporine (STS), a wide spectrum inhibitor of protein kinase. As well as the case of ER stress condition, TRB3 exerted the anti-apoptotic effect on STS-treated cells at least in my condition (Figure S11A), and in which TRB3 cleavage was also hardly observed (Figure S11B and C), even though STS-induced apoptosis is essentially mediated by CASP9 [34] that has TRB3 cleavage ability (Figure 1C). These results support my hypothesis that the anti-apoptotic effect of TRB3 is exerted during adaptive phase of stress as long as TRB3 is not cleaved. Taken together, my findings indicate that TRB3 has dual function – both in cell survival and also in apoptosis. This dual function of TRB3 might have contributed to the previously reported controversial role of TRB3 in apoptosis.

Initiator caspases, especially CASP8, CASP9, and CASP10, are known to play important roles in the beginning of apoptotic signal transduction [35]. Activated initiator caspases could then lead to the activation of downstream, effector caspases (i.e. CASP3, CASP6, and CASP7). Most caspases, including CASP8, CASP9, and CASP10 are predominantly located in the cytoplasm, and not in the nucleus [36,37]. Using fluorescence resonance energy transfer (FRET) technique it was shown that during the apoptotic process CASP3 activation is first initiated in the cytoplasm and then in the nucleus [25]. These results suggest that the cytoplasmic initiator caspases cannot easily activate the nuclear proCASP3. In fact, my results showed that expression of the nuclear proCASP3 (proCASP3-NLS-EmGFP) did not enhance

cell death under apoptotic conditions compared with control (DsRed-NLS), although expression of the cytoplasmic proCASP3 (proCASP3-EmGFP) enhanced it markedly (Figure 5). I found that TRB3 expression can induce cytoplasmic-to-nuclear translocation of proCASP3 under ER stress condition (Figure 4). TRB3 is a stress-inducible protein, and stress response is a mechanism by which cells adapt to stressful situations. Thus, TRB3 might insulate proCASP3 by promoting its entry into the nucleus to prevent CASP3 activation in the cytoplasm under TRB3-inducing stress conditions. Taken together, these results suggest that the overall CASP3 activity is regulated not only by proteolytic activation of proCASP3 but also by its subcellular distribution. To the best of my knowledge, TRB3-mediated nuclear translocation of proCASP3 is the first evidence supporting the above idea. However, I could not confirm the direct interaction between TRB3 and proCASP3 either by *in vitro* binding assay or by immunoprecipitation using the overexpressing cells. Further studies are required for better understanding of the mechanism.

My results indicated that TRB3 behaved as both an anti-apoptotic and a pro-apoptotic factor by whether or not TRB3 is cleaved by caspases under stressful situations. I propose the following model for the stress response mechanism of TRB3 (Figure S12). During the adaptive phase of stress, expressed TRB3 prevents CASP3 activation by nuclear translocation of proCASP3, which in turn leads to an extended adaptive phase and cell survival (Figure 3 and 4). However, when the stress becomes overwhelming, such as under prolonged stress, TRB3 is cleaved by caspases. According to indirect evidence, cleavage of TRB3 could be a trigger for further activation of caspases and thereby induces apoptosis (Figure 2), even if the condition that a part of proCASP3 had been localized to the nucleus by TRB3 (Figure 4A). Therefore, it seems like the anti-apoptotic effect of TRB3 had been abrogated when caspase activity is beyond tolerance level by lethal apoptotic stimuli such as TNFα/CHX unlike tunicamycin.

During ER stress, “because the UPR controls cell fate by switching between pro-survival and pro-apoptotic signaling, it is crucial to understand the parameters or events defining this transition, as well as gain insights on the components involved in its regulation” [12]. The exact mechanism controlling the transition between the adaptive and cell death programs is not well

understood. In this study, I propose that TRB3 functions as a stress sensor that detects caspase activity and also as a switch molecule that assists cells to commit to either survival or apoptotic pathway, and these functions of TRB3 are exerted through its own cleavage by caspases depending on the cellular context. Thus, TRB3 may play an important role in this strategic commitment mechanism.

Recently, it has been reported that CASP3 have cellular functions other than apoptosis, such as in cell development and differentiation [35]. In fact, during the development of iPS cells, CASP3/8 were activated and cleaved retinoblastoma protein (Rb), a known transcription coactivator [38]. The cleavage of Rb by CASP3/8 enhanced iPS formation. Among the initiator caspases, proCASP2 has been identified in the cell nucleus [39,40]. This raises a possibility that proCASP3 is actually activated in the nucleus via the mediation of TRB3, and that transcriptional regulators, such as Rb, could be targets of the nuclear form of active CASP3 under nonlethal condition (i.e. TRB3 non-cleavable conditions for nonapoptotic function). Alternatively, apoptosis accompanied by iPS formation is also suggestive of pro-apoptotic effect of TRB3. In another report, designed ER stress enhanced differentiation-associated apoptosis of myoblasts [41]. It is likely that ER stress-induced apoptosis selectively eliminates vulnerable cells. Interestingly, surviving myoblasts were resistant to apoptosis and they differentiated well. This result could be related to my finding that ER stress-induced TRB3 expression exerted anti-apoptotic effect by translocating proCASP3 into the nucleus. Because TRB3 expression is induced by various types of stresses, these results suggest that proCASP3 localizes in the nucleus under a variety of stress conditions. That proCASP3 was found to be localized in the nucleus, could now open avenues for finding new insights on biological roles of CASP3.

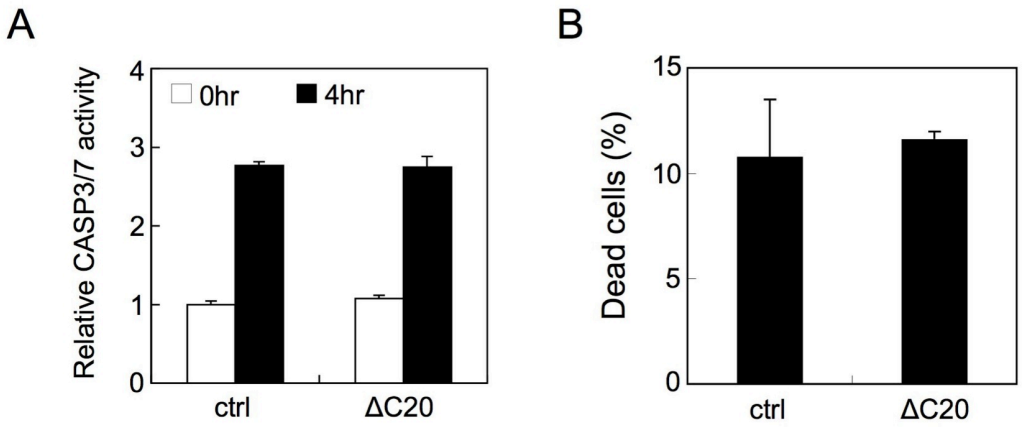

Figure S9 Expression of V5-ΔC20-TRB3 did not affect CASP3/7 activation and apoptosis. (A) HeLa cells were transfected with the V5-ΔC20-TRB3 expression plasmid. Twenty-four hours after, cells were treated with TNFα/CHX for 4 hr. CASP3/7 activity was measured in V5-ΔC20-TRB3 expressing HeLa cells as described in the legend of Figure 2C. Error bars indicate mean ± SD of three independent experiments. (B) Twenty-four hours after transfection with the V5-ΔC20-TRB3 expression plasmid or control vector, HeLa cells were treated with TNFα/CHX for 4 hr. The resulting dead cells were counted by trypan blue staining. Error bars indicate mean ± SD of three independent experiments.

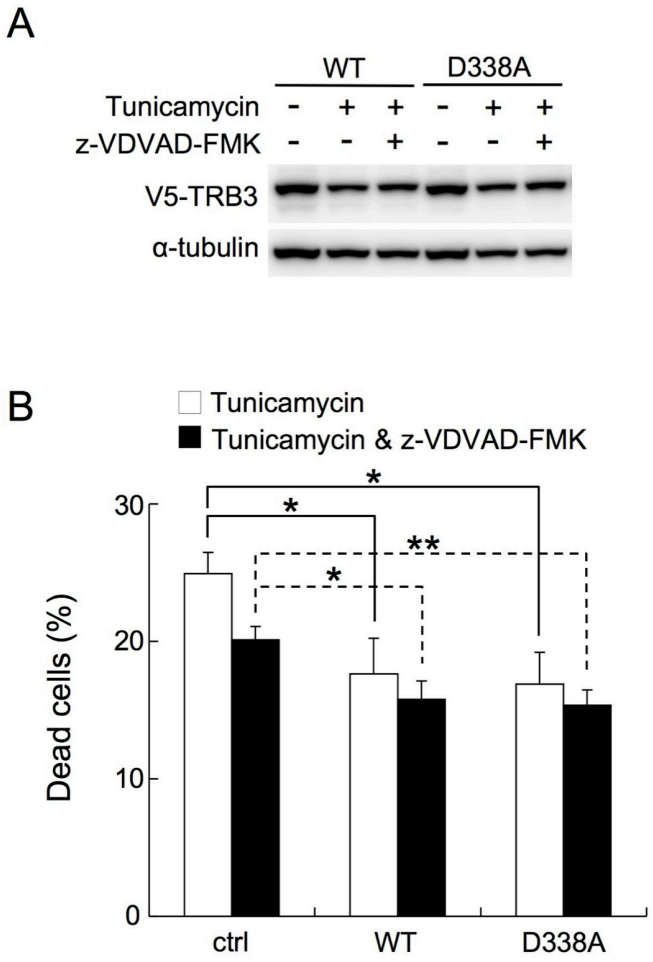

Figure S10 The effect of CASP2 on TRB3 under ER stress condition. Twenty-four hours after transfection with the indicated V5-TRB3 expression plasmid or control vector, HeLa cells were treated with tunicamycin in the absence or presence of CASP2 inhibitor z-VDVAD-FMK (10 μM) (BioVision) for 24 hr. The cell lysates were subjected to immunoblot analysis using anti-V5 antibody (A). Alternatively, the resulting dead cells were counted by trypan blue staining (B). Error bars indicate mean ± SD of four independent experiments. *P<0.005, ** P<0.001.

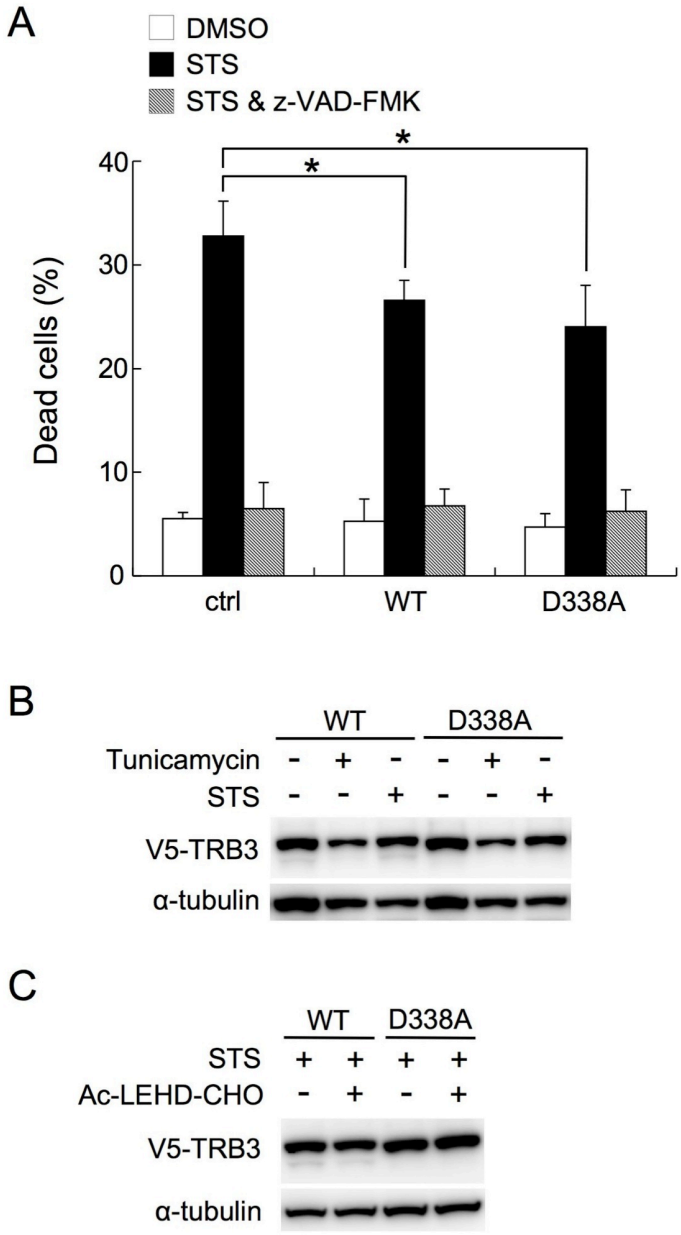

Figure S11 The effect of TRB3 on ER stress independent apoptosis induced by staurosporine. Twenty-four hours after transfection with the indicated V5-TRB3 expression plasmid or control vector, HeLa cells were treated with staurosporine (STS) (50 nM) (Wako Pure Chemical Industries, Osaka, Japan) for 24 hr. The resulting dead cells were counted by trypan blue staining (A). Error bars indicate mean ± SD of four independent experiments. *P<0.005. Alternatively, the cell lysates were subjected to immunoblot analysis using anti-V5 antibody. Tunicamycin (5 μM) (B) or CASP9 inhibitor Ac-LEHD-CHO (10 μM) (Calbiochem) (C) was used for a comparison analysis of TRB3 cleavage.

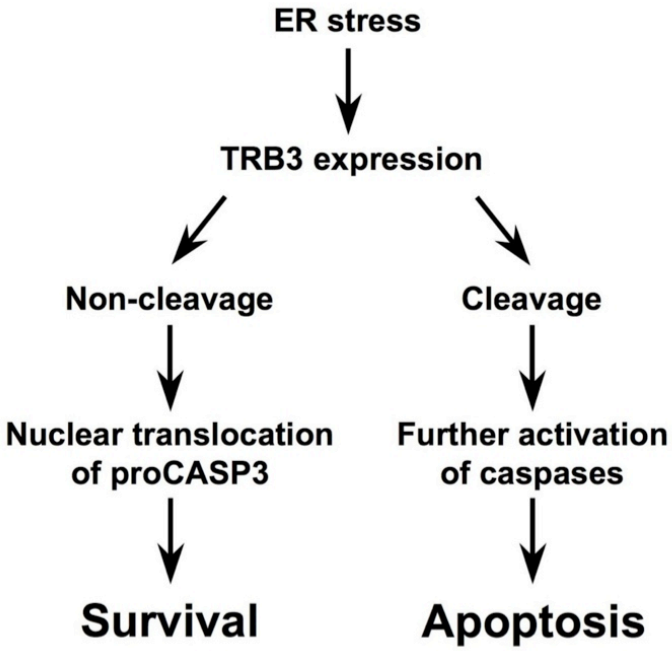

Figure S12 A hypothetical model for the stress response mechanism of TRB3.

5. REFERENCES

[1] Bowers, A.J., Scully, S. and Boylan, J.F. (2003). SKIP3, a novel Drosophila tribbles ortholog, is overexpressed in human tumors and is regulated by hypoxia. Oncogene 22, 2823-35.

[2] Du, K., Herzig, S., Kulkarni, R.N. and Montminy, M. (2003). TRB3: a tribbles homolog that inhibits Akt/PKB activation by insulin in liver. Science 300, 1574-7.

[3] Kato, S. and Du, K. (2007). TRB3 modulates C2C12 differentiation by interfering with Akt activation. Biochem Biophys Res Commun 353, 933-8.

[4] Kiss-Toth, E. et al. (2004). Human tribbles, a protein family controlling mitogen-activated protein kinase cascades. J Biol Chem 279, 42703-8.

[5] Ord, D. and Ord, T. (2003). Mouse NIPK interacts with ATF4 and affects its transcriptional activity. Exp Cell Res 286, 308-20.

[6] Ohoka, N., Yoshii, S., Hattori, T., Onozaki, K. and Hayashi, H. (2005). TRB3, a novel ER stress-inducible gene, is induced via ATF4-CHOP pathway and is involved in cell death. EMBO J 24, 1243-55.

[7] Bezy, O., Vernochet, C., Gesta, S., Farmer, S.R. and Kahn, C.R. (2007). TRB3 blocks adipocyte differentiation through the inhibition of C/EBPbeta transcriptional activity. Mol Cell Biol 27, 6818-31.

[8] Takahashi, Y., Ohoka, N., Hayashi, H. and Sato, R. (2008). TRB3 suppresses adipocyte differentiation by negatively regulating PPARgamma transcriptional activity. J Lipid Res 49, 880-92.

[9] Qi, L. et al. (2006). TRB3 links the E3 ubiquitin ligase COP1 to lipid metabolism. Science 312, 1763-6.

[10] Xu, C., Bailly-Maitre, B. and Reed, J.C. (2005). Endoplasmic reticulum stress: cell life and death decisions. J Clin Invest 115, 2656-64.

[11] Yoshida, H. (2007). ER stress and diseases. FEBS J 274, 630-58.

[12] Woehlbier, U. and Hetz, C. (2011). Modulating stress responses by the UPRosome: A matter of life and death. Trends Biochem Sci 36, 329-37.

[13] Jousse, C. et al. (2007). TRB3 inhibits the transcriptional activation of stress-regulated genes by a negative feedback on the ATF4 pathway. J Biol Chem 282, 15851-61.

[14] Puthalakath, H. et al. (2007). ER stress triggers apoptosis by activating BH3-only protein Bim. Cell 129, 1337-49.

[15] Galehdar, Z., Swan, P., Fuerth, B., Callaghan, S.M., Park, D.S. and Cregan, S.P. (2010). Neuronal apoptosis induced by endoplasmic reticulum stress is regulated by ATF4-CHOP-mediated induction of the Bcl-2 homology 3-only member PUMA. J Neurosci 30, 16938-48.

[16] Zou, C.G., Cao, X.Z., Zhao, Y.S., Gao, S.Y., Li, S.D., Liu, X.Y., Zhang, Y. and Zhang, K.Q. (2009). The molecular mechanism of endoplasmic reticulum stress-induced apoptosis in PC-12 neuronal cells: the protective effect of insulin-like growth factor I. Endocrinology 150, 277-85.

[17] Schwarzer, R., Dames, S., Tondera, D., Klippel, A. and Kaufmann, J. (2006). TRB3 is a PI 3-kinase dependent indicator for nutrient starvation. Cell Signal 18, 899-909.

[18] Corcoran, C.A., Luo, X., He, Q., Jiang, C., Huang, Y. and Sheikh, M.S. (2005). Genotoxic and endoplasmic reticulum stresses differentially regulate TRB3 expression. Cancer Biol Ther 4, 1063-7.

[19] Inoue, S., Browne, G., Melino, G. and Cohen, G.M. (2009). Ordering of caspases in cells undergoing apoptosis by the intrinsic pathway. Cell Death Differ 16, 1053-61.

[20] Würstle, M.L., Laussmann, M.A. and Rehm, M. (2010). The caspase-8 dimerization/dissociation balance is a highly potent regulator of caspase-8, -3, -6 signaling. J Biol Chem 285, 33209-18.

[21] Tadokoro, D., Takahama, S., Shimizu, K., Hayashi, S., Endo, Y. and Sawasaki, T. (2010). Characterization of a caspase-3-substrate kinome using an N- and C-terminally tagged protein kinase library produced by a cell-free system. Cell Death Dis 1, e89.

[22] Ohoka, N., Sakai, S., Onozaki, K., Nakanishi, M. and Hayashi, H. (2010). Anaphase-promoting complex/cyclosome-cdh1 mediates the ubiquitination and degradation of TRB3. Biochem Biophys Res Commun 392, 289-94.

[23] Mancini, M., Nicholson, D.W., Roy, S., Thornberry, N.A., Peterson, E.P., Casciola-Rosen, L.A. and Rosen, A. (1998). The caspase-3 precursor has a cytosolic and mitochondrial distribution: implications for apoptotic signaling. J Cell Biol 140, 1485-95.

[24] Kamada, S., Kikkawa, U., Tsujimoto, Y. and Hunter, T. (2005). Nuclear translocation of caspase-3 is dependent on its proteolytic activation and recognition of a substrate-like protein(s). J Biol Chem 280, 857-60.

[25] Takemoto, K., Nagai, T., Miyawaki, A. and Miura, M. (2003). Spatio-temporal activation of caspase revealed by indicator that is insensitive to environmental effects. J

Cell Biol 160, 235-43.

[26] Ord, D., Meerits, K. and Ord, T. (2007). TRB3 protects cells against the growth inhibitory and cytotoxic effect of ATF4. Exp Cell Res 313, 3556-67.

[27] Wali, V.B., Bachawal, S.V. and Sylvester, P.W. (2009). Endoplasmic reticulum stress mediates gamma-tocotrienol-induced apoptosis in mammary tumor cells. Apoptosis 14, 1366-77.

[28] Humphrey, R.K., Newcomb, C.J., Yu, S.M., Hao, E., Yu, D., Krajewski, S., Du, K. and Jhala, U.S. (2010). Mixed lineage kinase-3 stabilizes and functionally cooperates with TRIBBLES-3 to compromise mitochondrial integrity in cytokine-induced death of pancreatic beta cells. J Biol Chem 285, 22426-36.

[29] Szegezdi, E., Logue, S.E., Gorman, A.M. and Samali, A. (2006). Mediators of endoplasmic reticulum stress-induced apoptosis. EMBO Rep 7, 880-5.

[30] Misiti, F., Sampaolese, B., Pezzotti, M., Marini, S., Coletta, M., Ceccarelli, L., Giardina, B. and Clementi, M.E. (2005). Abeta(31-35) peptide induce apoptosis in PC 12 cells: contrast with Abeta(25-35) peptide and examination of underlying mechanisms. Neurochem Int 46, 575-83.

[31] Giri, K., Ghosh, U., Bhattacharyya, N.P. and Basak, S. (2003). Caspase 8 mediated apoptotic cell death induced by beta-sheet forming polyalanine peptides. FEBS Lett 555, 380-4.

[32] Cheung, H.H., Lynn Kelly, N., Liston, P. and Korneluk, R.G. (2006). Involvement of caspase-2 and caspase-9 in endoplasmic reticulum stress-induced apoptosis: a role for the IAPs. Exp Cell Res 312, 2347-57.

[33] Upton, J.P., Austgen, K., Nishino, M., Coakley, K.M., Hagen, A., Han, D., Papa, F.R. and Oakes, S.A. (2008). Caspase-2 cleavage of BID is a critical apoptotic signal downstream of endoplasmic reticulum stress. Mol Cell Biol 28, 3943-51.

[34] Manns, J. et al. (2011). Triggering of a novel intrinsic apoptosis pathway by the kinase inhibitor staurosporine: activation of caspase-9 in the absence of Apaf-1. FASEB J 25, 3250-61.

[35] Launay, S., Hermine, O., Fontenay, M., Kroemer, G., Solary, E. and Garrido, C. (2005). Vital functions for lethal caspases. Oncogene 24, 5137-48.

[36] Zhivotovsky, B., Samali, A., Gahm, A. and Orrenius, S. (1999). Caspases: their intracellular localization and translocation during apoptosis. Cell Death Differ 6, 644-51.

[37] Shikama, Y., U, M., Miyashita, T. and Yamada, M. (2001). Comprehensive studies on subcellular localizations and cell death-inducing activities of eight GFP-tagged apoptosis-related caspases. Exp Cell Res 264, 315-25.

[38] Li, F. et al. (2010). Apoptotic caspases regulate induction of iPSCs from human fibroblasts. Cell Stem Cell 7, 508-20.

[39] Colussi, P.A., Harvey, N.L. and Kumar, S. (1998). Prodomain-dependent nuclear localization of the caspase-2 (Nedd2) precursor. A novel function for a caspase prodomain. J Biol Chem 273, 24535-42.

[40] Mancini, M., Machamer, C.E., Roy, S., Nicholson, D.W., Thornberry, N.A., Casciola-Rosen, L.A. and Rosen, A. (2000). Caspase-2 is localized at the Golgi complex and cleaves golgin-160 during apoptosis. J Cell Biol 149, 603-12.

[41] Nakanishi, K., Dohmae, N. and Morishima, N. (2007). Endoplasmic reticulum stress increases myofiber formation in vitro. FASEB J 21, 2994-3003.

CHAPTER II

Nek5, a novel substrate for caspase-3, promotes skeletal muscle differentiation by up-regulating caspase activity

SUMMARY

Accumulating evidence suggests that caspase-3-mediated cleavage of protein kinase could be a key event to regulate cell differentiation. In this study, I investigated the role of Nek5 kinase, identified as a novel substrate for caspase-3, in skeletal muscle differentiation. Up-regulation of Nek5 mRNA expression was accompanied by cell differentiation. The myotube formation was promoted in Nek5 expressing cells, and conversely, which was inhibited in Nek5 knockdown cells. Furthermore, I found that caspase-3 activity, an important factor for myogenic differentiation, was enhanced by Nek5 cleavage. Although caspase-3-cleaved Nek5 partially exerted promyogenic effect, it tended to induce apoptotic cell death. In summary, my findings suggest that Nek5 promotes myogenic differentiation through up-regulation of caspase activity.

Abbreviations: DM, differentiation medium; GM, growth medium; MHC, myosin heavy chain; MRFs, myogenic regulatory factors

1. INTRODUCTION

Controlling the myogenic differentiation is an essential task for embryonic muscle development and homeostasis of muscle tissue in post-developmental stage. Myogenesis is a multistep process, in which proliferating mononucleated myoblasts withdraw from the cell cycle, followed by differentiation into myocytes and fusion into multinucleated myotubes to form functional muscle fibers [1-3]. The myogenic program is regulated by sequential activation of myogenic regulatory factors (MRFs), the basic helix–loop–helix (bHLH) family of transcription factors (Myf5, MyoD, myogenin and MRF4), which can induce expression of muscle-specific genes in concert with transcriptional cofactors, MEF2 and E proteins [4-8].

Apoptosis, a physiological process of programmed cell death, plays a crucial role in organogenesis during development [9]. Myogenic differentiation is actually accompanied by typical apoptotic signaling events such as caspase-3 activation, and subpopulation of myoblasts undergoes developmental apoptosis [10]. Caspase-3 activation leads to not only apoptosis but also a non-apoptotic process of differentiation [11]. Although the mechanism by which caspase-3 promotes differentiation is still unclear, several studies have suggested that the effects produced by caspase-dependent cleavage of selected substrates, especially some protein kinases (such as MST1 and HPK1), are required for the regulation of differentiation [10,12-14]. It is noteworthy that active MST1 mediated by caspase-3 partially overcomes the resistance to the skeletal muscle differentiation of caspase-3 null myoblasts [10]. Activation of Rho-kinase, a caspase-targeted kinase, is also required for myogenesis [15]. However, regardless of the caspase involvement, kinases play significant roles in myogenesis. For example, ERK5 regulates the process of cell fusion in skeletal muscle differentiation through Klf transcription factors, independently of the activities of MyoD and MEF2 family transcription factors [16]. Other reports have shown that p38 MAPK induces skeletal muscle gene expression by activating MRFs and MEF2 transcriptional activities, and chromatin remodeling activities on muscle-specific promoters [17].

We previously identified 30 protein kinases as novel substrates for caspase-3 [18], and investigated the role of them in skeletal muscle differentiation. Nek5, a newly identified

caspase-3 substrate, belongs to the NIMA (never in mitosis A)-related kinase (Nek) family that is involved in cell cycle regulation. Its function, however, remains to be defined [19]. In this report, I demonstrate that Nek5 is involved in the promotion of myogenic differentiation by up-regulating the caspase activity.

2. MATERIALS AND METHODS

2.1. Reagents and antibodies

Tumor necrosis factor-α (TNFα) (Calbiochem, La Jolla, CA) was used together with cycloheximide (CHX) (Chemicon, Temecula, CA) to induce apoptosis. The broad-spectrum caspase inhibitor Z-VAD-FMK (Peptide Institute Inc., Osaka, Japan) or the reversible inhibitor of caspase-3/7, 5-[(S)-(+)2-(methoxymethyl)pyrrolidino]sulfonylisatin (Calbiochem) was supplemented with TNFα/CHX. Antibodies against the following antigens were used: myosin heavy chain (MHC) (clone MF20, Developmental Studies Hybridoma Bank, Iowa City, IA), troponin C (Santa Cruz Biotechnology, Santa Cruz, CA), GFP (clone 1E4, Medical & Biological Laboratories Co, Ltd., Nagoya, Japan), V5 epitope (Invitrogen, Carlsbad, CA), α-tubulin (clone DM1A, Sigma, St. Louis, MO), FLAG epitope (clone M2, Sigma), cleaved caspase-3 (clone 5A1E, Cell Signaling Technology, Beverly, MA) and cleaved PARP (Cell Signaling Technology). Alexa Fluor 488-conjugated streptavidin was purchased from Invitrogen.

2.2. Plasmid constructs

To construct expression plasmid for mammalian cells, cDNAs encoding human MyoD1 (RefSeq: NM_002478), mouse Nek5 (RefSeq: NM_177898) and mouse Nek2 (RefSeq: NM_010892) were subcloned into suitable vectors from pcDNA series (pcDNA3.1/nV5-DEST, pcDNA3.2/V5-DEST, pcDNA6.2/N-EmGFP-DEST and pcDNA6.2/C-EmGFP-DEST) (Invitrogen) by recombination using Gateway® system. A point mutant of Nek5 (serine 438 to aspartic acid, i.e. D438A) was generated by site-directed mutagenesis using a PrimeSTAR mutagenesis basal kit (Takara Bio Inc., Otsu, Japan). For knockdown analysis, RNA interference (RNAi) was performed using pcDNA6.2-GW/EmGFP-miR expression vector (Invitrogen) that enables to identify artificial microRNA (miR) expressing cells by co-cistronic expression of EmGFP. The following sequences were selected as RNAi targets: 5'-CCAATATCGTAACCTTCTTCA-3' (miR-Nek5-#1), 5'-GGGTTTCTTTCAGGATGTCAT-3' (miR-Nek5-#2) and

5'-CCTGGCTAGTGTCATTTCAAA-3' (miR-Nek2) corresponding to the nucleotide sequences in the coding regions of Nek5 and Nek2, respectively. The pcDNA6.2-GW/EmGFP-miR-neg control plasmid (Invitrogen) containing a non-target sequence was used as a negative control (miR-NC).

2.3. Cell culture and transfection

C2/4 [20], a subclone of the C2C12 mouse myoblast cell line, was referred to simply as C2C12 in this paper. C2C12 cells and HeLa cells were maintained at 37˚C in a 5% CO_2 incubator in a growth medium (GM) of Dulbecco's modified eagle medium (DMEM) (Nissui, Tokyo, Japan) supplemented with 10% fetal bovine serum (Sigma), 2 mM L-glutamine (GIBCO, Grand Island, NY), and antibiotics (100 units/ml penicillin and 100 μg/ml streptomycin) (GIBCO). Myogenic differentiation of C2C12 myoblasts was induced by replacing the GM with a differentiation medium (DM) that is DMEM with high glucose (Wako, Osaka, Japan) supplemented with 2% horse serum and penicillin-streptomycin. Unless otherwise noted, cells were cultured in GM. All transfections in this study, except for the experiment in Figure 4A (Lipofectamine 2000, Invitrogen), were performed using the TransIT-LT1 transfection reagent (Mirus, Madison, WI) according to the manufacturer's instruction.

2.4. Western blot analysis

All Western blot analyses were performed as described previously [21]. Briefly, proteins in whole-cell lysates were separated by SDS-PAGE and transferred onto a PVDF membrane by electroblotting. After blocking with 5% milk/TBST, the membrane was probed with a given primary antibody and then incubated with a horseradish peroxidase (HRP)-conjugated secondary antibody. The immunoreactive proteins were visualized using Immobilon Western HRP substrate Luminol Reagent (Millipore, Bedford, MA) and LAS-4000 mini biomolecular imager (GE Healthcare, Piscataway, NJ).

2.5. Immunostaining analysis

Cells were fixed with 4% paraformaldehyde in phosphate-buffered saline (PBS) for 15 min at room temperature, and then permeabilized with 0.5% Triton X-100 in PBS for 5 min. After blocking with 5% calf serum in TBST for 1 hr, the cells were incubated with anti-troponin C antibody, anti-MHC antibody or anti-cleaved caspase-3 antibody for 1 hr at 37 ˚C. The cells were then incubated with Alexa Fluor 555-conjugated appropriate secondary antibody (Invitrogen) for 1 hr at room temperature. Fluorescence images were acquired by the Carl Zeiss LSM710 confocal laser scanning microscope (Carl Zeiss, Jena, Germany).

2.6. Real-time quantitative RT-PCR analysis

Total cellular RNA was extracted from C2C12 cells using a QIAeasy RNA mini kit (Qiagen, Valencia, CA). Extracted total RNA was subjected to reverse transcription with a Transcriptor First Strand cDNA Synthesis Kit (Roche, Basel, Schweiz). The real-time qRT-PCR analysis was performed using a LightCycler 480 Real-time PCR System (Roche). The following primer set for Nek5 was designed by the software of Assay Design Center (Roche): 5'-ggaagaacaaaatgaaggacca-3' (forward) and 5'-cttcatgtcgttgtggtactgtt-3' (reverse). The values were normalized to GAPDH (primer set was purchased from Roche).

2.7. Cell-free protein synthesis and in vitro cleavage assay

Construction of DNA template and cell-free transcription/translation for Nek5 were performed as described previously [18]. Cleavage reaction of the synthesized Nek5 by caspase was also carried out following the method described previously [21].

2.8. Luminometric detection of caspase-3/7 activity

Caspase-3/7 activity was measured by using the luminometric Caspase-Glo® 3/7 Assay kit (Promega, Madison, WI) and a GloMaxTM 96 Microplate Luminometer (Promega) according to the manufacturer's instructions.

2.9. Statistical analysis

Data shown are mean ± SD. Student's t-test was used to determine the significance of differences. *P* values of less than 0.05 were considered statistically significant.

3. RESULTS

3.1. Nek5 is a novel substrate for caspase-3

We previously reported a high-throughput protease substrate screening method by which 30 kinases were identified as novel substrates for caspase-3 [18]. Here, using the same method, I identified Nek5 as a substrate for caspase-3, but not caspase-6, -7 and -8 (Figure 1A). Caspase-3 prefers an Asp residue at both P1 and P4 positions in DXXD motif for proteolytic cleavage [22]. Although three preferred motifs were indeed found in Nek5, a potential cleavage site was speculated at Asp438/Arg439 from the molecular weight of the cleaved fragment as estimated by Western blot analysis (Figure 1A, arrowheads, and Figure 1B). To precisely determine the cleavage site, I constructed mutants of Nek5 as shown in Figure 1B: alanine point mutant (D438A) and deletion mutant (ΔC176, amino acids 1-438). *In vitro* cleavage assay revealed that D438A-Nek5 and ΔC176-Nek5 were not cleaved by caspase-3, whereas wild type Nek5 (WT) was cleaved (Figure 1C). Additionally, the size of cleaved fragment derived from WT-Nek5 was almost the same with that of ΔC176-Nek5. A similar result was obtained in apoptotic HeLa cells (Figure 1D). An increase in the amount of cleaved fragment was observed in apoptosis induction using TNFα/CHX, and both the pan-caspase inhibitor Z-VAD-FMK and caspase-3/7 inhibitor completely blocked it (Figure 1D and E). These results clearly indicate that Nek5 is cleaved at Asp438 by caspase-3 during the apoptotic process.

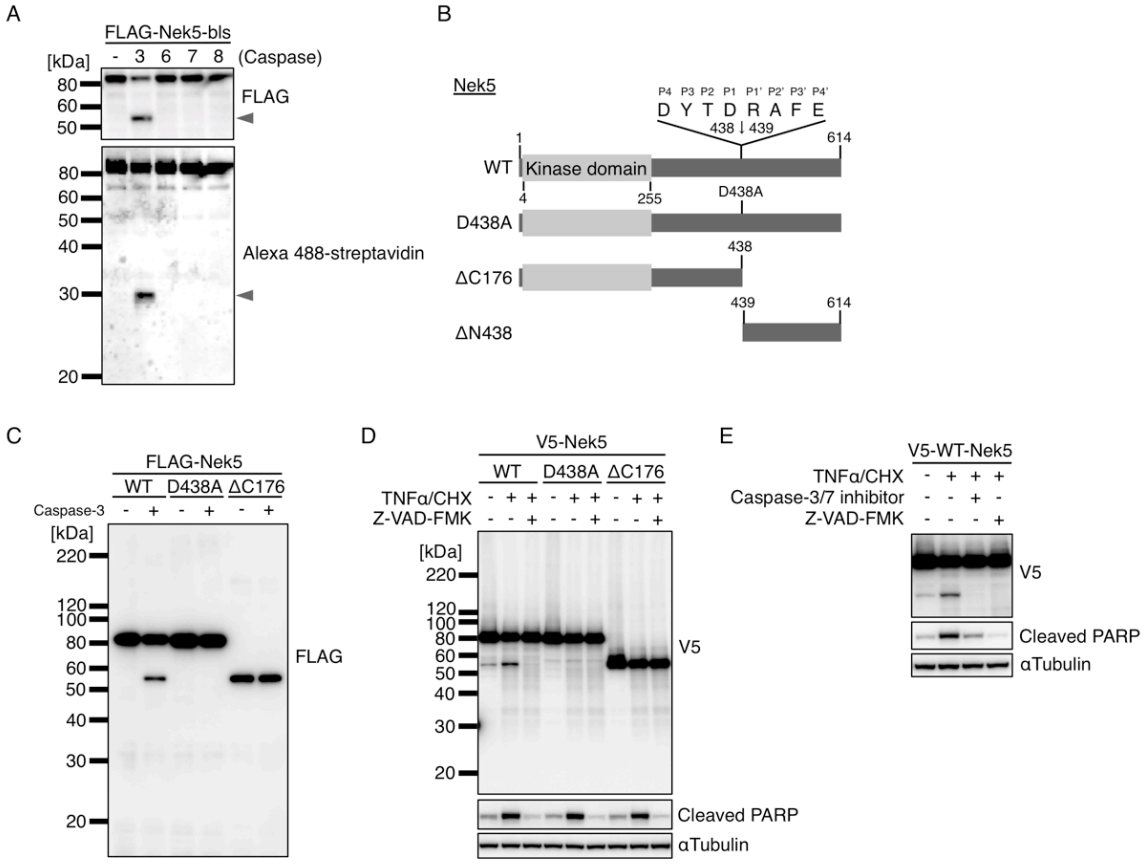

Figure 1. Nek5 is cleaved by caspase-3 *in vitro* and in apoptotic cells. (A) N-terminal FLAG tagged and C-terminal biotinylated Nek5 (FLAG-Nek5-bls) was synthesized by the wheat cell-free expression system. Nek5 was incubated in the presence (+) or absence (-) of indicated caspase and the cleavage product was then detected using the anti-FLAG antibody (upper panel) and Alexa 488-conjugated streptavidin (lower panel), which bound to the N- and C-termini, respectively. Arrowheads indicate the cleaved fragments. (B) Schematic diagram of Nek5 constructs used in this study and the cleavage site for caspase-3. WT, wild type Nek5; D438A, caspase-3 cleavage-site mutant of Nek5; ΔC176, deletion mutant containing the kinase domain (amino acids 1-438); and ΔN438, deletion mutant (amino acids 439-614). (C) Each FLAG-Nek5 synthesized by the wheat cell-free expression system was incubated in the presence (+) or absence (-) of caspase-3, and then detected using the anti-FLAG antibody. (D) Twenty-four hours after transfection of HeLa cells with the indicated V5-tagged Nek5 expression plasmid, cells were treated with TNFα (20 ng/ml)/CHX (100 μM) in the presence or absence of Z-VAD-FMK (100 μM) for 4 hr. Cell lysates were subjected to Western blot analysis using anti-V5, anti-cleaved PARP (apoptosis marker) and anti-α-Tubulin (internal control) antibodies. (E) The reversible inhibitor of caspase-3/7, 5-[(S)-(+)2-(methoxymethyl)pyrrolidino]sulfonylisatin (100 μM) was used as in Figure 1D.

3.2. Nek5 promotes myogenic differentiation of C2C12 myoblasts

Accumulating evidence suggests that protein kinases as substrates for caspase-3 play a significant role in regulation of differentiation [10,11,13]. To investigate the possible role of Nek5 in myogenic differentiation, Nek5 was transiently overexpressed in C2C12 myoblasts. The expression levels of the two myogenic markers: myosin heavy chain (MHC) and troponin C, were increased by Nek5 expression compared to EGFP-V5 (transfection control) (Figure 2A). A muscle-specific regulator MyoD1 is known to induce myogenesis in numerous cell types including C2C12 cells [23]. Immunostaining showed that large myotubes were formed in cells expressing Nek5 (Figure 2B). Furthermore, Nek5 was mostly expressed in the differentiated cells that were positive for MHC expression, and was hardly found in myoblasts negative for MHC, as is the case with MyoD1 (Figure 2C). These results indicate that Nek5 is able to promote myogenic differentiation.

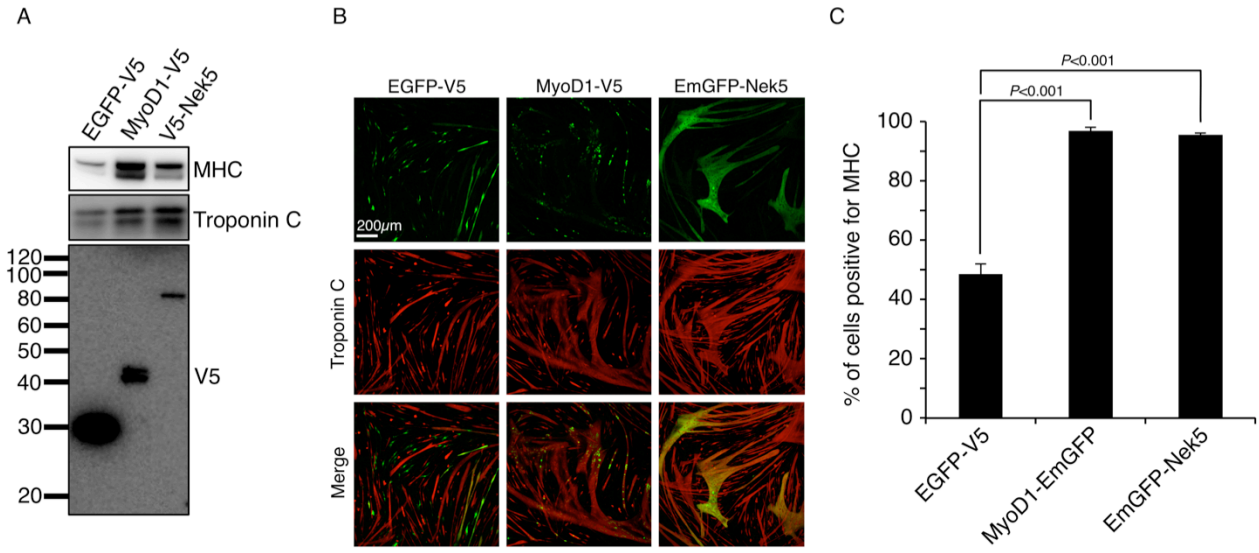

Figure 2. Nek5 exerts a promyogenic effect. C2C12 cells were transfected with the indicated expression vectors. (A) After 3 days of transfection, cell lysate were subjected to Western blot analysis using anti-MHC, anti-troponin C, and anti-V5 antibodies, respectively. (B) After 6 days of transfection, differentiated cells were detected by immunostaining with anti-troponin C (red). Scale bars = 200 μm. (C) Differentiated cells were immunostained with an anti-MHC antibody after 4 days of transfection, and then quantified for the percentage of that in cells expressing the indicated proteins. Error bars indicate SD (N=4, each N consists of 150 < cells). A *P* value <0.05 was accepted as significant.

3.3. Up-regulation of Nek5 expression during differentiation contributes to the promyogenic effect

To investigate whether Nek5 expression is induced during myogenic differentiation, I monitored the expression levels of Nek5 mRNA. The induction of differentiation in C2C12 cells by differentiation medium (DM) resulted in a transient increase in the expression of Nek5 mRNA (Figure 3A). A significant increase in Nek5 mRNA was observed in C2C12 cells cultured in growth medium (GM) on day 4 (Figure 3A, right panel), which was consistent with the timing of a dramatic increase in the expression of MHC mRNA (Figure 3B). These results suggest that myogenic differentiation is accompanied by up-regulation of Nek5. Next, to examine whether Nek5 expression is required for the progression of myogenic differentiation, I constructed vectors expressing microRNAs (miRNA) targeting Nek5 (miR-Nek5-#1 and miR-Nek5-#2). These miRNAs specifically suppressed exogenous Nek5 expression (Figure S1). However, due to the unavailability of a specific antibody and/or the significantly low expression of Nek5 protein, I could not conclude that whether or not the expression of endogenous Nek5 is down-regulated in C2C12 cells. The vectors enable visualization of miRNA-expressing cells by co-cistronic expression of EmGFP. Among them, a population of troponin C negative regarded as undifferentiated cells was frequently observed in cells suppressing Nek5 expression compared with non-target negative control miRNA (miR-NC) and Nek2 (miR-Nek2) (Figure 3C). To further confirm it, percentage of differentiated cells expressing miRNA was quantified by MHC staining, and the results showed that the percentage was decreased in cells expressing miRNA-Nek5 (Figure 3D). Taken together, my results suggest that Nek5 expression contributes to the progression of myogenic differentiation.

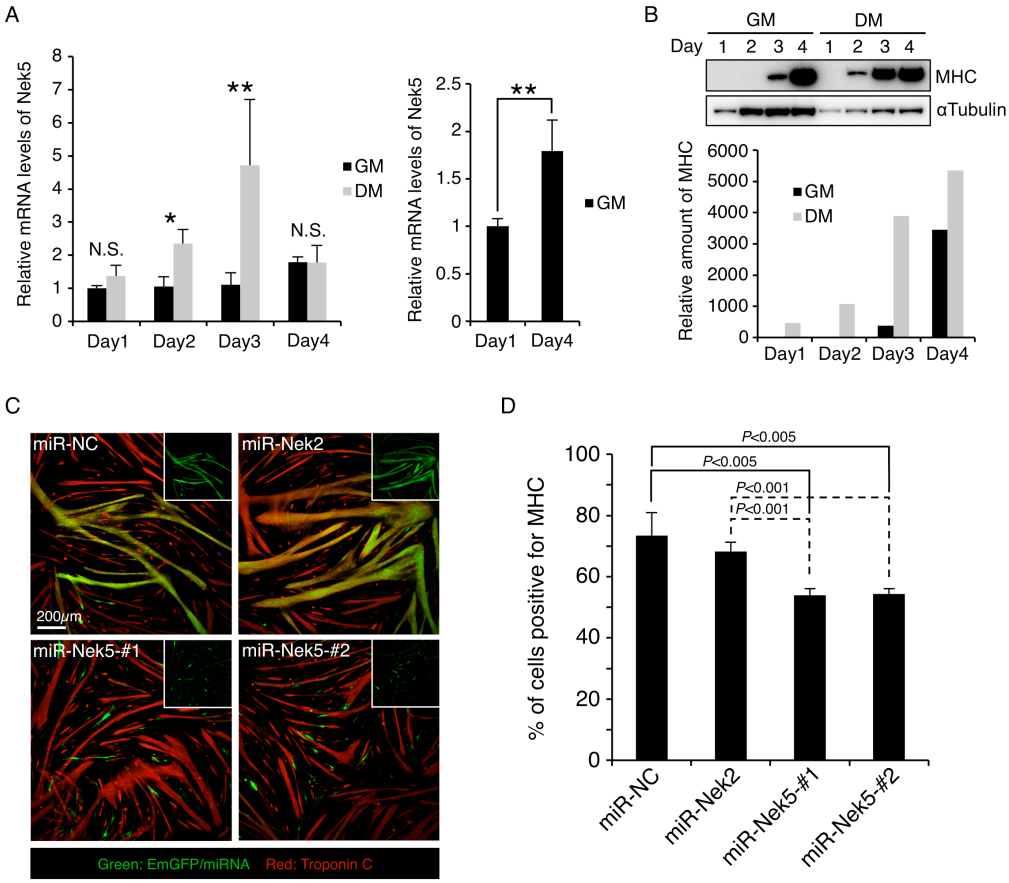

Figure 3. The mRNA encoding Nek5 is up-regulated during myogenic differentiation. (A, B) Semi-confluent C2C12 cells were cultured in growth medium (GM) or differentiation medium (DM) for indicated days, and then collected. (A) The relative expression levels of Nek5 mRNA were determined by real-time quantitative RT-PCR. GAPDH mRNA was used as an internal control. Error bars indicate SD (N=3). **P*<0.001, ***P*<0.005, statistically significant difference. N.S., not significant. (B) Cell lysates were subjected to Western blot analysis using the anti-MHC antibody. The relative expression levels of MHC protein were quantified using ImageJ software. α-tubulin was used for normalization. (C, D) C2C12 cells were transfected with the indicated artificial miRNA expression plasmids. (C) After 6 days of transfection, differentiated cells were detected by immunostaining with an anti-troponin C (red). Scale bars = 200 μm. (D) Differentiated cells were immunostained with an anti-MHC antibody after 4 days of transfection, and then quantified for the percentage of that in miRNA-expressing cells of inner panel visualized by co-cistronic expression of EmGFP. Error bars indicate SD (N=4, each N consists of 150 < cells).

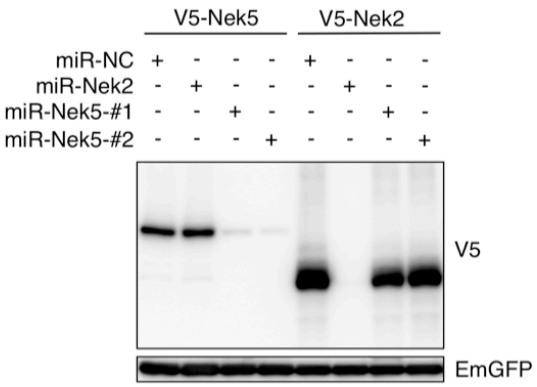

Figure S1. Artificial miRNAs targeting Nek5 mRNA specifically suppress exogenous Nek5 expression. HeLa cells were co-transfected with the indicated expression vectors, and then cultured for 24 hr. The cell lysates were subjected to Western blot analysis using anti-V5 and anti-GFP antibodies. The expression of each miRNA was detected by co- cistronic expression of EmGFP.

3.4. Nek5 is involved in the regulation of caspase-3 activity during myogenic differentiation

Previous studies have suggested that caspase-mediated cleavage of kinase could be a key signal for regulation of cell differentiation [10,12-14]. For example, caspase-3-dependent activation of MST1 brings about promyogenic effect as well as apoptosis [10]. In this study, I demonstrated that Nek5 is a substrate for caspase-3 as show in Figure 1. Since activation of caspase-3 is known to be associated with myogenic differentiation, I tested whether the cleavage of Nek5 indeed occurs during the differentiation process. In WT-Nek5, instead of D438A mutant that is resistant to proteolytic cleavage by caspase-3, a remarkable reduction of full-length Nek5 and the appearance of the cleaved fragment were clearly observed on Day1 but not Day2 by replacing the GM with DM (Figure 4A). This is likely to be the result of caspase-3 activity that is transiently increased and reaches the peak level within 24 hours after induction of myogenic differentiation in C2C12 myoblasts [10]. Thus, this result suggests that the physiological processing of Nek5 occurs in the early phase of myogenic differentiation. I next asked whether the cleavage of Nek5 has some implications for myogenesis. The large fragment of Nek5 (ΔC176-Nek5) produced by caspase-3 contains the kinase domain, which is raising the possibility that the kinase activity of Nek5 is modulated by the cleavage, as is the case for MST1 [10]. To address this possibility, a conventional kinase assay using histone H1 and myelin basic protein as substrates was performed. However, no difference in the kinase activity was found between full-length Nek5 and the cleaved fragment. Nevertheless, caspase-3-mediated cleavage of substrates is often linked to the pro-apoptotic effect [24]. Therefore, to test whether the cleaved fragment of Nek5 can exert pro-apoptotic effect, caspase-3/7 activity was measured in HeLa cells expressing ΔC176-Nek5. As shown in Figure 4B, increase in the caspase-3/7 activity was observed in cells expressing ΔC176-Nek5. Interestingly, WT-Nek5 and D438A-Nek5 also exerted the pro-apoptotic effect compared with EGFP-V5 as a control (Figure 4B). As expected, these levels of caspase-3/7 activity were correlated with the number of apoptotic cells (Figure 4C and D). Moreover, to verify whether Nek5 was involved in the activation of caspase-3 during myogenic differentiation, knockdown

of Nek5 expression was performed in C2C12 myoblasts. In consequence of that, caspase-3 activation was partially inhibited in cells suppressing Nek5 expression (Figure 4E and F). It seems that the modest inhibition is due to low transfection efficiency of miRNA expression plasmids. Alternatively, in order to get the maximal effect of Nek5 knockdown, myogenic differentiation was induced in DM instead of GM, and then caspase-3 activity was detected at the time point of caspase-3 activity peak. But, unexpectedly, the effect was more modest. This may be the result of a drastic increase in caspase-3 activity, which negates the effect of Nek5 knockdown. Thus, these results suggest that the cleavage of Nek5 enhances the pro-apoptotic effect of Nek5 in the process of myogenic differentiation. In the last analysis, to assess how the Nek5-dependent regulation of caspase activity affects myogenic differentiation, the degree of differentiation in cells expressing WT-Nek5 and its mutants was estimated and compared by counting the number of nuclei in C2C12 myotubes. In any case, each Nek5 serves as a positive regulator for the progression of myogenic differentiation compared with control (Figure 4G). However, large myotubes (more than 15 nuclei) were not observed in cells expressing ΔC176-Nek5 so many as the case of WT-Nek5 and D438A-Nek5. This result is consistent with the relative expression levels of MHC (Figure S2). Taken together, these findings suggest a possibility that the level of caspase activity due to ΔC176-Nek5 preferentially leads to apoptosis rather than promyogenic effect. Therefore, Nek5 may contribute to the fine-tuning of caspase activity suitable for myogenesis.

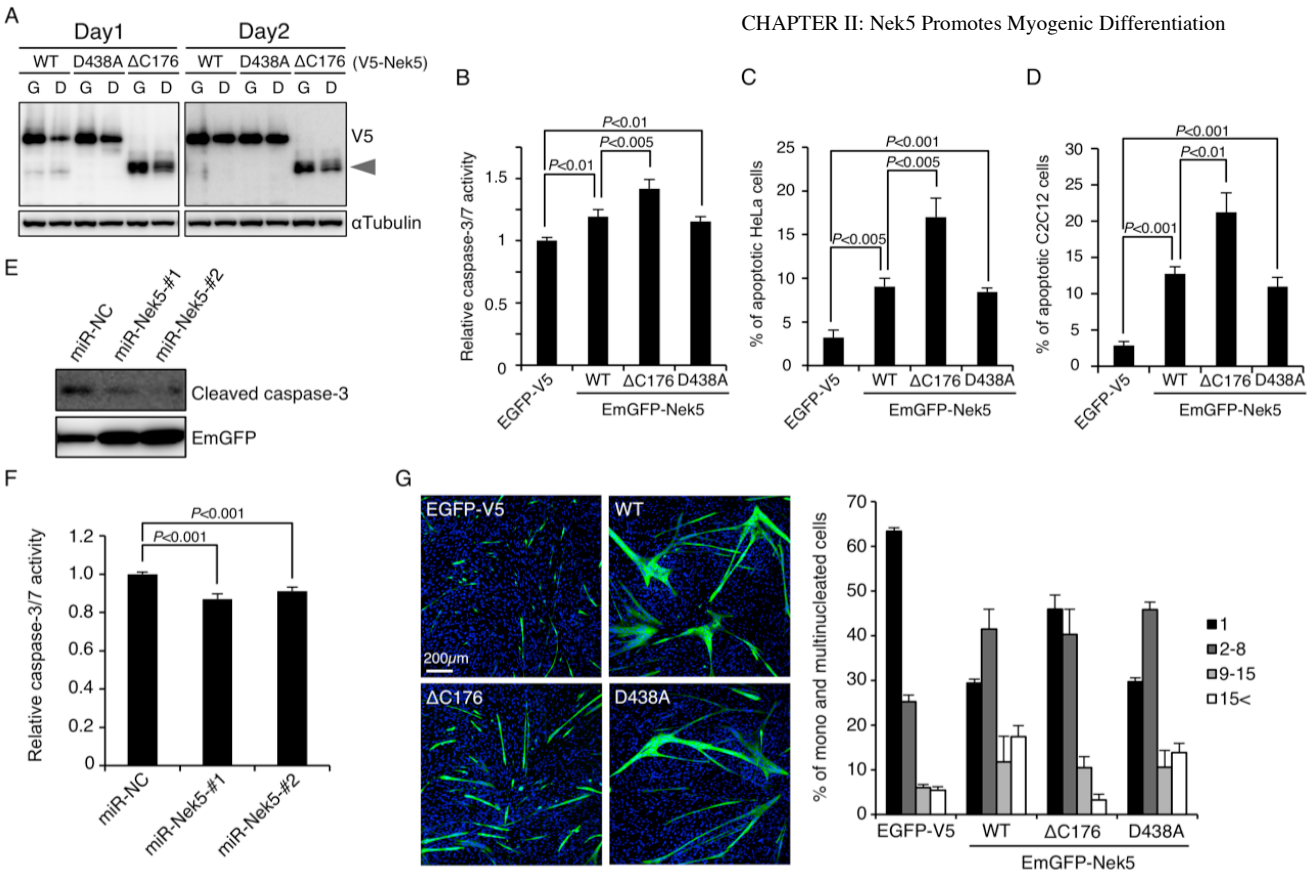

Figure 4. Nek5 regulates caspase-3 activity during myogenic differentiation. (A) Twenty-four hours after transfection, C2C12 cells were further cultured in fresh GM or DM for 1 day or 2 days. The cell lysates were subjected to Western blot analysis using anti-V5 and anti-α-Tubulin antibodies. Arrowhead indicates the location of cleaved fragments. (B) HeLa cells were cultured for 2 days after transfection, and then caspase-3/7 activity was measured. Error bars indicate SD (N=3). (C) Thirty hours after transfection, HeLa cells were immunostained with an anti-cleaved caspase-3 antibody and counterstained with DAPI to visualize the nuclei. Apoptotic cells were counted among cells expressing the indicated proteins. Cells fulfilling all of the following features were defined as apoptotic cells: cleaved caspase-3 positive, cell shrinkage and nuclear condensation and/or fragmentation. Error bars indicate SD (N=3, each N consists of 200 < cells). (D) Apoptotic C2C12 cells were counted as in Figure 4C without immunofluorescent staining of cleaved caspase-3. Error bars indicate SD (N=3, each N consists of 100 < cells). (E, F) After 3 days of transfection, C2C12 cells were collected. Cell lysates were subjected to Western blot analysis (E) and luminometric assay (F) to detect caspase-3 activity. Error bars indicate SD (N=4). (G) After 4 days of transfection, C2C12 cells were stained with DAPI (blue, left panel) to count nuclei of cells expressing the indicated proteins (green, left panel). The number of nuclei was grouped into four categories (1, 2-8, 9-15, 15<), and the percentage of that was quantified (right panel). Error bars indicate SD (N=3, each N consists of 100 < cells).

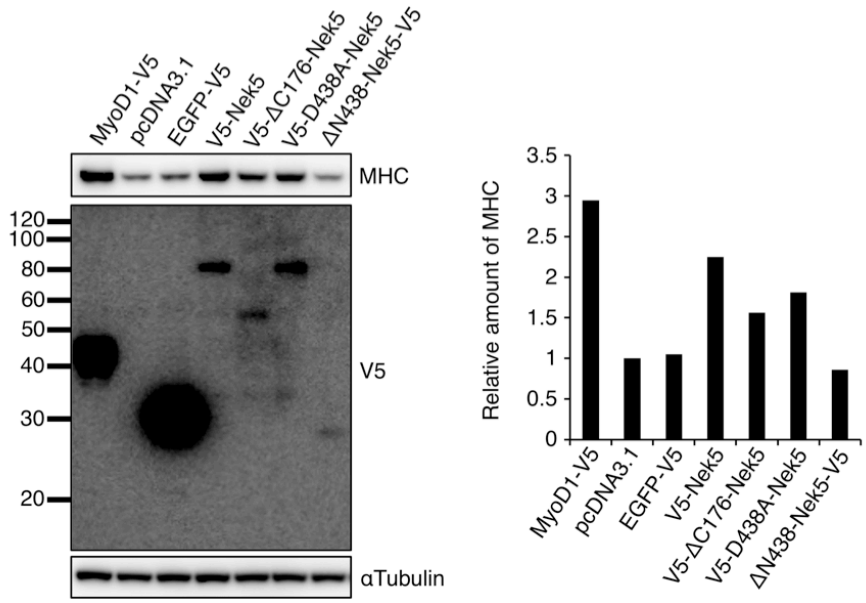

Figure S2. The promyogenic effect of Nek5 and its mutants. C2C12 cells were transfected with the indicated expression vectors and pcDNA3.1 empty vector as a control. After 4 days of transfection, cell lysates were subjected to Western blot analysis using anti-MHC, anti- V5 and anti-α-Tubulin (internal control) antibodies. Representative data from two experiments are shown (left panel). The relative expression levels of MHC protein were quantified using ImageJ software (right panel). α-tubulin was used for normalization.

4. DISCUSSION

Studies in the last decade or so have demonstrated that mammalian Nek kinases mainly function as cell cycle regulators. However, function of Nek5 remains unknown. In this study, I present evidence that Nek5 is involved in myogenic differentiation by controlling caspase-3 activity.

The regulation of caspase-3 activity is capable of realizing the non-apoptotic outcomes, such as a departure from self-renewing state of embryonic stem cells or progenitor (i.e. differentiation) [25], and nuclear reprogramming in iPS cells induction (i.e. dedifferentiation) [26]. Defects in these processes including myogenic differentiation were observed in cells lacking caspase-3 or under inhibitory conditions of caspase-3 activity due to the biological and chemical barrier [10,27]. As regards the role of caspase-3 signaling in cell differentiation, Larsen's study showed the possibility that caspase-3/caspase-activated DNase (CAD)-dependent DNA strand breaks promote cell differentiation by modifying the DNA/nuclear microenvironment to regulate gene expression, such as p21 [28]. Furthermore, Fernando and Arnold demonstrated that caspase-3-dependent activation of MST1 and HPK1 kinases mediates pro-apoptotic and pro-survival signaling, respectively, which contributes to progression of differentiation [10,13].

As shown in Figure 1 and 4, my data revealed that Nek5 is a substrate for caspase-3 and is able to exert pro-apoptotic and promyogenic effects. Although the mechanism by which pro-apoptotic effect of Nek5 was produced remains unclear, caspase-3-mediated cleavage would enhance it. However, it seems that not all of the processing accelerates myogenesis, because the promyogenic effect of ΔC176-Nek5 was lower than WT-Nek5 and D438A-Nek5 (Figure 4G and Figure S2). Additionally, the promyogenic effect was not observed in cells expressing ΔN438-Nek5 (amino acids 439-614, see Figure 1B). Alternatively, I have eliminated the possibility that the promyogenic effect is dependent on kinase activity, since no difference was observed between WT-Nek5 and ΔC176-Nek5. Recently, Nakanishi et al. proposed that ER stress exerts a positive effect on myofiber formation by eliminating vulnerable cells to make a resistant cell population that are competent to efficiently fuse with one another, and/or

drawing the potential for differentiation from myoblasts [29]. In murine models, ER stress-induced apoptosis but not by membrane- or mitochondrial-targeted apoptotic signals was specifically mediated by caspase-12 [30]. Under conditions of myogenic differentiation, in fact, caspase-12 was activated by ER stress [31]. Taken together with above reports, my findings indicate that Nek5 contributes to the fine-tuning of caspase activity to realize the suitable environment for myogenesis.

5. REFERENCES

[1] Hanzlíková, V., Macková, E.V. and Hník, P. (1975). Satellite cells of the rat soleus muscle in the process of compensatory hypertrophy combined with denervation. Cell Tissue Res 160, 411-21.

[2] Abmayr, S.M. and Pavlath, G.K. (2012). Myoblast fusion: lessons from flies and mice. Development 139, 641-56.

[3] Bentzinger, C.F., Wang, Y.X. and Rudnicki, M.A. (2012). Building muscle: molecular regulation of myogenesis. Cold Spring Harb Perspect Biol 4

[4] Murre, C., McCaw, P.S. and Baltimore, D. (1989). A new DNA binding and dimerization motif in immunoglobulin enhancer binding, daughterless, MyoD, and myc proteins. Cell 56, 777-83.

[5] Wright, W.E., Sassoon, D.A. and Lin, V.K. (1989). Myogenin, a factor regulating myogenesis, has a domain homologous to MyoD. Cell 56, 607-17.

[6] Megeney, L.A. and Rudnicki, M.A. (1995). Determination versus differentiation and the MyoD family of transcription factors. Biochem Cell Biol 73, 723-32.

[7] Puri, P.L. and Sartorelli, V. (2000). Regulation of muscle regulatory factors by DNA-binding, interacting proteins, and post-transcriptional modifications. J Cell Physiol 185, 155-73.

[8] Lassar, A.B., Davis, R.L., Wright, W.E., Kadesch, T., Murre, C., Voronova, A., Baltimore, D. and Weintraub, H. (1991). Functional activity of myogenic HLH proteins requires hetero-oligomerization with E12/E47-like proteins in vivo. Cell 66, 305-15.

[9] Kerr, J.F., Wyllie, A.H. and Currie, A.R. (1972). Apoptosis: a basic biological phenomenon with wide-ranging implications in tissue kinetics. Br J Cancer 26, 239-57.

[10] Fernando, P., Kelly, J.F., Balazsi, K., Slack, R.S. and Megeney, L.A. (2002). Caspase 3 activity is required for skeletal muscle differentiation. Proc Natl Acad Sci U S A 99, 11025-30.

[11] Fernando, P. and Megeney, L.A. (2007). Is caspase-dependent apoptosis only cell differentiation taken to the extreme? FASEB J 21, 8-17.

[12] Kanuka, H., Kuranaga, E., Takemoto, K., Hiratou, T., Okano, H. and Miura, M. (2005). Drosophila caspase transduces Shaggy/GSK-3beta kinase activity in neural precursor development. EMBO J 24, 3793-806.

[13] Arnold, R., Frey, C.R., Müller, W., Brenner, D., Krammer, P.H. and Kiefer, F. (2007).

Sustained JNK signaling by proteolytically processed HPK1 mediates IL-3 independent survival during monocytic differentiation. Cell Death Differ 14, 568-75.

[14] Fernando, P., Brunette, S. and Megeney, L.A. (2005). Neural stem cell differentiation is dependent upon endogenous caspase 3 activity. FASEB J 19, 1671-3.

[15] Sordella, R., Jiang, W., Chen, G.C., Curto, M. and Settleman, J. (2003). Modulation of Rho GTPase signaling regulates a switch between adipogenesis and myogenesis. Cell 113, 147-58.

[16] Sunadome, K., Yamamoto, T., Ebisuya, M., Kondoh, K., Sehara-Fujisawa, A. and Nishida, E. (2011). ERK5 regulates muscle cell fusion through Klf transcription factors. Dev Cell 20, 192-205.

[17] Lluís, F., Perdiguero, E., Nebreda, A.R. and Muñoz-Cánoves, P. (2006). Regulation of skeletal muscle gene expression by p38 MAP kinases. Trends Cell Biol 16, 36-44.

[18] Tadokoro, D., Takahama, S., Shimizu, K., Hayashi, S., Endo, Y. and Sawasaki, T. (2010). Characterization of a caspase-3-substrate kinome using an N- and C-terminally tagged protein kinase library produced by a cell-free system. Cell Death Dis 1, e89.

[19] Moniz, L., Dutt, P., Haider, N. and Stambolic, V. (2011). Nek family of kinases in cell cycle, checkpoint control and cancer. Cell Div 6, 18.

[20] Yoshida, S., Fujisawa-Sehara, A., Taki, T., Arai, K. and Nabeshima, Y. (1996). Lysophosphatidic acid and bFGF control different modes in proliferating myoblasts. J Cell Biol 132, 181-93.

[21] Shimizu, K., Takahama, S., Endo, Y. and Sawasaki, T. (2012). Stress-Inducible Caspase Substrate TRB3 Promotes Nuclear Translocation of Procaspase-3. PLoS One 7, e42721.

[22] Cryns, V. and Yuan, J. (1998). Proteases to die for. Genes Dev 12, 1551-70.

[23] Davis, R.L., Weintraub, H. and Lassar, A.B. (1987). Expression of a single transfected cDNA converts fibroblasts to myoblasts. Cell 51, 987-1000.

[24] Kurokawa, M. and Kornbluth, S. (2009). Caspases and kinases in a death grip. Cell 138, 838-54.

[25] Fujita, J., Crane, A.M., Souza, M.K., Dejosez, M., Kyba, M., Flavell, R.A., Thomson, J.A. and Zwaka, T.P. (2008). Caspase activity mediates the differentiation of embryonic stem cells. Cell Stem Cell 2, 595-601.

[26] Li, F. et al. (2010). Apoptotic caspases regulate induction of iPSCs from human fibroblasts. Cell Stem Cell 7, 508-20.

[27] Hunt, L.C., Upadhyay, A., Jazayeri, J.A., Tudor, E.M. and White, J.D. (2011). Caspase-3, myogenic transcription factors and cell cycle inhibitors are regulated by leukemia inhibitory factor to mediate inhibition of myogenic differentiation. Skelet Muscle 1, 17.

[28] Larsen, B.D., Rampalli, S., Burns, L.E., Brunette, S., Dilworth, F.J. and Megeney, L.A. (2010). Caspase 3/caspase-activated DNase promote cell differentiation by inducing DNA strand breaks. Proc Natl Acad Sci U S A 107, 4230-5.

[29] Nakanishi, K., Dohmae, N. and Morishima, N. (2007). Endoplasmic reticulum stress increases myofiber formation in vitro. FASEB J 21, 2994-3003.

[30] Nakagawa, T., Zhu, H., Morishima, N., Li, E., Xu, J., Yankner, B.A. and Yuan, J. (2000). Caspase-12 mediates endoplasmic-reticulum-specific apoptosis and cytotoxicity by amyloid-beta. Nature 403, 98-103.

[31] Nakanishi, K., Sudo, T. and Morishima, N. (2005). Endoplasmic reticulum stress signaling transmitted by ATF6 mediates apoptosis during muscle development. J Cell Biol 169, 555-60.

CONCLUSIONS

In this thesis, I have consistently focused on how caspase-mediated cleavage of kinases regulates apoptosis and cell differentiation. In CHAPTER I, I revealed that TRB3 behaves as both an anti-apoptotic and a pro-apoptotic protein by whether or not TRB3 is cleaved by caspases under stressful situations. In the case of non-cleavable conditions represented by ER stress, TRB3 exerted anti-apoptotic effect by promoting procaspase-3 entry into the nucleus. This is a novel anti-apoptotic mechanism based on caspase distribution (Shimizu et al: *PLoS ONE*, 2012). In CHAPTER II, I found that Nek5 and its cleavage contribute to the fine-tuning of caspase activity to provide the suitable environment for myogenesis. This is the first evidence of Nek5 that plays an important role in mammalian cells (Shimizu and Sawasaki: *FEBS Letters*, 2013).

Although the mechanism is still unclear, both TRB3 and Nek5 cleavage were involved in the up-regulation of caspase-3 activity without alterations in kinase activity. These cleavages were important event for cell fate determination between cell survival and apoptosis or differentiation. Therefore, to understand the complicated mechanisms of apoptosis and differentiation, it will be necessary to clarify the physiological role of caspase-dependent cleavage of more substrates in addition to protein kinase.

ACKNOWLEDGMENTS

I wish to express my most sincere gratitude to Professor Tatsuya Sawasaki for the useful comments, remarks and encouragement throughout the learning process of this thesis. He continually and convincingly conveyed a spirit of adventure and an excitement in regard to research. Without his guidance and persistent help this dissertation would not have been possible.

I would like to thank my mentorship of Dr. Shokichi Takahama for his guidance, valuable discussions and persistent help.

I would also like to thank Professor Yaeta Endo, Assistant Professor Hiroyuki Takeda, Assistant Professor Hirotaka Takahashi, Mr. Tatsuya Akagi and Mr. Daisuke Tadokoro for their guidance and encouragement.

I thank laboratory members and all members of Department of Applied Chemistry, Faculty of Engineering, Ehime University.

Special thanks must be given to Professor Atsuko Sehara (Kyoto University) and Associate Professor Kazuhiro Sakamaki (Kyoto University) for kindly providing the C2/4 (C2C12) cells and a mutant caspase-3 cDNA clone, respectively.

This work was supported by a Grant-in-Aid for JSPS Fellows from Japan Society for the Promotion of Science as a PI.

Finally, I wish to express my deepest gratitude to my parents for all supports throughout my student life.